ISSN 2538-1016; 58

NEW ZEALAND
DEPARTMENT OF SCIENTIFIC AND INDUSTRIAL RESEARCH
BULLETIN 202

Hydrological Studies in the New Zealand Region 1966 and 1967

Oceanic Hydrology North-West of New Zealand

Hydrology of the North-East Tasman Sea

by

D. M. GARNER

New Zealand Oceanographic Institute, Wellington

New Zealand Oceanographic Institute
Memoir No. 58

1970

NEW ZEALAND
DEPARTMENT OF SCIENTIFIC AND INDUSTRIAL RESEARCH
BULLETIN 202

Hydrological Studies in the New Zealand Region 1966 and 1967

Oceanic Hydrology North-West of New Zealand

Hydrology of the North-East Tasman Sea

by

D. M. GARNER

New Zealand Oceanographic Institute, Wellington

New Zealand Oceanographic Institute
Memoir No. 58

1970

***Price** $1.50*

This work is licensed under the Creative Commons Attribution-NonCommercial-NoDerivs 3.0 Unported License.
To view a copy of this license, visit http://creativecommons.org/licenses/by-nc-nd/3.0/

This publication should be referred to as:

Bull. N.Z. Dep. scient. ind. Res. 202

MS Completed for Publication: October 1968

© Crown Copyright 1970

A. R. SHEARER, GOVERNMENT PRINTER, WELLINGTON, NEW ZEALAND—1970

This work is licensed under the Creative Commons Attribution-NonCommercial-NoDerivs 3.0 Unported License.
To view a copy of this license, visit http://creativecommons.org/licenses/by-nc-nd/3.0/

FOREWORD

Reconnaissance studies of the hydrology of the ocean areas around New Zealand were given priority in the early research programmes carried out by the Institute.

Since 1963 this work has been followed by detailed studies of the summer situation in specific areas of the New Zealand region. The results presented in this memoir extend our knowledge of ocean water circulation to the areas north and west of the North Island.

J. W. BRODIE, Director,

New Zealand Oceanographic Institute.

Inset 1

This work is licensed under the Creative Commons Attribution-NonCommercial-NoDerivs 3.0 Unported License.
To view a copy of this license, visit http://creativecommons.org/licenses/by-nc-nd/3.0/

CONTENTS

Oceanic Hydrology North-west of New Zealand

Tables

Figures

Hydrology Of The North-east Tasman Sea

This work is licensed under the Creative Commons Attribution-NonCommercial-NoDerivs 3.0 Unported License.
To view a copy of this license, visit http://creativecommons.org/licenses/by-nc-nd/3.0/

CONTENTS—*continued*

Tables

Figures

This work is licensed under the Creative Commons Attribution-NonCommercial-NoDerivs 3.0 Unported License.
To view a copy of this license, visit http://creativecommons.org/licenses/by-nc-nd/3.0/

OCEANIC HYDROLOGY NORTH-WEST OF NEW ZEALAND

by

D. M. Garner

New Zealand Oceanographic Institute

ABSTRACT

A survey of ocean temperature and salinity during February 1966, the fourth of a series, is described for the region between the north of New Zealand and the vicinity of Norfolk Island.

Geopotential calculations showed a net east-going geostrophic flow through the survey area above the core of the Antarctic Intermediate Water at a depth of about 1 km. A large wave in this flow, probably topographically induced, appeared to the east of the Norfolk Ridge. No indication of a Tropical Convergence or of a south-west-flowing Trade Drift was found.

Calculations of sound velocity showed a belt of relatively high velocity running zonally through the middle of the survey area in the axis of the SOFAR channel. Velocity corrections for echo soundings were derived for the region.

INTRODUCTION

SURVEY DETAILS

A survey of the temperature and salinity of ocean waters north-west of New Zealand was undertaken by the New Zealand Oceanographic Institute from m.v. *Taranui* during February 1966. This cruise was the fourth in a series of hydrological surveys designed to provide a representation of the summer hydrological situation in oceanic waters around New Zealand. Previous cruises have covered the region east of the northern part of New Zealand (Garner, 1967a; Ridgway in press) and the south-east Tasman Sea (Garner, 1967b).

In Fig. 1 the station plan of the cruise is shown in relation to the main bathymetric features of the region surveyed. Four lines, each of six stations about 90 miles apart and approximately meridionally oriented, were worked between latitudes 27° and 35° S. The first two lines (Sta. E 496–501 and E 502–507) lay over the western and eastern sides of the New Caledonia Basin where the bottom slopes upwards to the Lord Howe Rise and the Norfolk Ridge, respectively. The other two lines (Sta. E 508–514–519) lay over the western and eastern margins, respectively, of the Norfolk Basin, which is flanked on the west by the Norfolk Ridge and on the east by the Three Kings Rise. The last two stations of the cruise were to the north-east of North Cape on the south-western margin of the South Fiji Basin.

At each station the vertical variation of temperature and salinity from the surface to a maximum depth of 2.5 km was measured using the bathythermograph, reversing bottles, and reversing thermometers as in the previous cruises of this series. Temperatures and pressures at sampling points were calculated from the reversing thermometer readings through the use of LaFond's (1951) tables and the thermometer certificates. Salinities of water samples drawn from the reversing bottles were determined at sea with an inductively coupled salinometer.

PRESENTATION OF DATA

The station circumstances (times, positions, weather) are listed in Table 1, and the station data (observed temperatures, depths, pressures and salinities, with derived values of density, geopotential anomaly and sound velocity) are listed in the Appendix. The tables of LaFond (1951), Bark *et al.* (1964), and the U.S. Navy Hydrographic Office (1956) were used for these derivations. Tracings of bathythermograph records are reproduced in Fig. 5. Distributions of temperature and salinity on various surfaces are mapped in Figs. 3–10 in support of the discussion following.

This work is licensed under the Creative Commons Attribution-NonCommercial-NoDerivs 3.0 Unported License.
To view a copy of this license, visit http://creativecommons.org/licenses/by-nc-nd/3.0/

DISCUSSION

GEOSTROPHIC CIRCULATION

Fig. 2 is a map of the dynamic topography of the survey area referred to an isobaric surface of 1,000 decibars. Essentially similarly shaped topography was obtained for the sea surface with respect to the 500, 1,000, 1,750, and 2,000 decibar surfaces, so evidently the choice of a reference surface is not critical for this region as it was, for instance, in the south-east Tasman Sea (Garner, 1967b). The 1,000 decibar reference surface has been chosen for the pattern reproduced here to facilitate comparison with other topographies published both in this series of studies and elsewhere.

If the reference surface be supposed level, the contours of dynamic height (Fig. 2) are also streamlines of the surface circulation that would be in geostrophic equilibrium with the observed density distribution. The net flow through the survey area at the surface (and, apparently, at all levels within the upper few hundred metres) was east-going at all latitudes. A large perturbation in this zonal flow occurred east of the Norfolk Ridge. While station spacing was too coarse to define the configuration of this feature uniquely, it has been depicted (Fig. 2) as a trough in the topography, the axis of which extended from west of North Island towards Norfolk Island. A relatively strong north-west-going stream, counter to the general trend, ran south of Norfolk Island for a short distance as part of this disturbance.

The relation of the topography of the survey area to that of the Pacific as a whole may be seen by comparing Fig. 2 with the work of Reid (1961, Fig. 1) or Wyrtki (1962b, Fig. 1). On the basis of these studies the survey area is seen to be situated on the southern slopes of a topographic ridge with its axis lying in the subtropics, approximately on the latitude of Fiji. Along the northern side of this ridge the South Equatorial Current flows westwards. The East Australian Current flows southwards along the Australian coast around the western end of this ridge, and the return flow of the South Pacific Subtropical Gyral

TABLE 1. Station Circumstances

Air (screen) temperature and wind properties were estimated at bridge level. Uncorrected depths were derived from an intermittently operating echo sounder.

Station No.	N.Z. Date/Time (1966 February)		Latitude °S	Longitude °E	Depth m	Air Temp. °C	Wind	
	Start	Finish					Dir. °T	Speed kts
E 496	10/1244	1455	35° 00′	166° 00′	2,350	21.0	040	14
E 497	11/1055	1328	33° 30′	164° 49′	3,065	21.1	280	35
E 498	12/0635	0949	31° 54′	164° 20′	..	21.9	265	4
E 499	12/1900	2055	30° 30′	164° 31′	..	23.0	calm	..
E 500	13/0615	0813	28° 59′	164° 24′	3,396	24.5	045	3
E 501	13/1812	1957	27° 30′	164° 30′	3,275	24.1	120	10
E 502	14/0929	1120	27° 30′	166° 30′	3,508	23.7	110	9
E 503	14/2140	2315	29° 00′	166° 32′	3,406	23.5	090	6
E 504	15/0825	1011	30° 30′	166° 29′	2,995	23.7	050	12
E 505	15/2120	2400	32° 00′	165° 53′	..	22.4	050	6
E 506	16/1025	1151	33° 30′	166° 28′	..	21.0	060	4
E 507	16/2210	2345	35° 00′	167° 30′	2,672	21.4	090	4
E 508	17/1703	1900	35° 00′	170° 30′	2,014	20.7	100	12
E 509	18/0848	1135	33° 00′	170° 18′	2,280	22.5	calm	..
E 510	18/2145	2335	32° 00′	169° 00′	..	23.6	040	9
E 511	19/1034	1353	30° 27′	168° 32′	..	24.2	020	11
E 512	20/0253	0504	28° 57′	168° 57′	3,250	24.3	055	5
E 513	21/0428	0806	27° 30′	169° 00′	..	25.7	090	12
E 514	21/2204	2343	26° 45′	170° 25′	..	25.9	080	13
E 515	22/1046	1216	27° 24′	171° 35′	..	25.5	090	16
E 516	22/2326	2453	29° 00′	171° 30′	..	23.6	090	5
E 517	23/1017	1200	30° 25′	171° 35′	..	23.5	090	3
E 518	23/2122	2347	32° 00′	172° 00′	..	22.8	calm	..
E 519	24/0900	1125	33° 24′	171° 33′	..	22.5	calm	..
E 520	25/0846	1021	33° 50′	173° 00′	..	22.0	calm	..
E 521	25/1540	1718	33° 50′	174° 00′	2,363	24.0	calm	..

This work is licensed under the Creative Commons Attribution-NonCommercial-NoDerivs 3.0 Unported License.
To view a copy of this license, visit http://creativecommons.org/licenses/by-nc-nd/3.0/

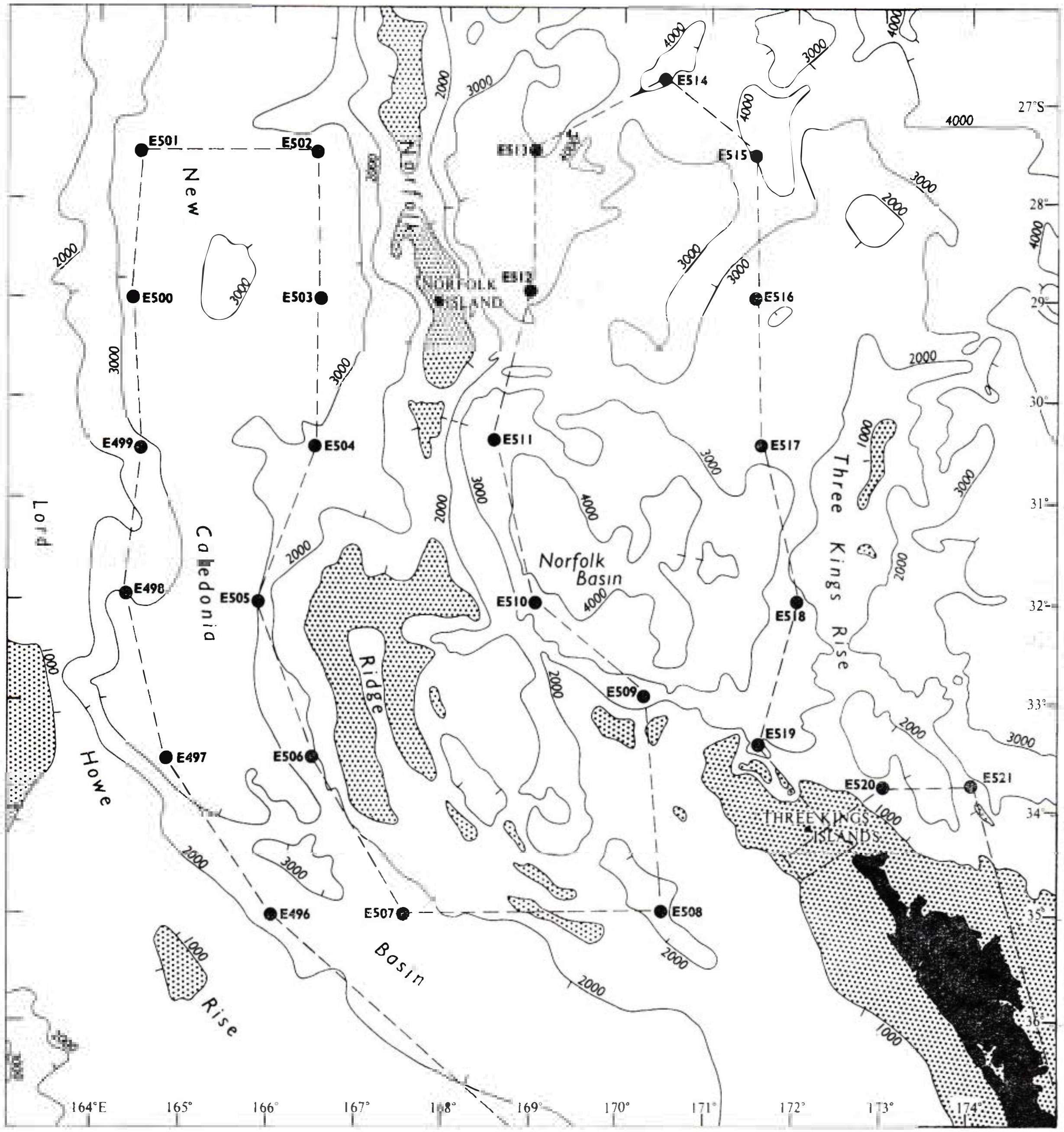

FIG. 1. The survey area north-west of New Zealand showing station positions against the bathymetry of the region. Isobaths are shown in metres at intervals of 1 km. Areas where the depth is less than 1 km are stippled. The cruise track is shown as a broken line.

system flows eastwards, to the north of New Zealand, along the southern slopes of the governing high. Surface geopotential anomalies accord well when comparing the present work with these broader schemes previously established, and thus it might be inferred that upper water layers of this survey were derived from the main outflow from the Tasman Sea of the East Australian Current.

Wyrtki (1962b) compared his topographic map of the south-west Pacific with charts of average surface currents derived from ships' reports, and found "good agreement south of 30° S and throughout the range of the East Australian Current". These average surface current charts, (for example, Wyrtki (1960) or Defant (1961, Plate 8)) show to the south of the relatively strong South Equatorial

This work is licensed under the Creative Commons Attribution-NonCommercial-NoDerivs 3.0 Unported License.
To view a copy of this license, visit http://creativecommons.org/licenses/by-nc-nd/3.0/

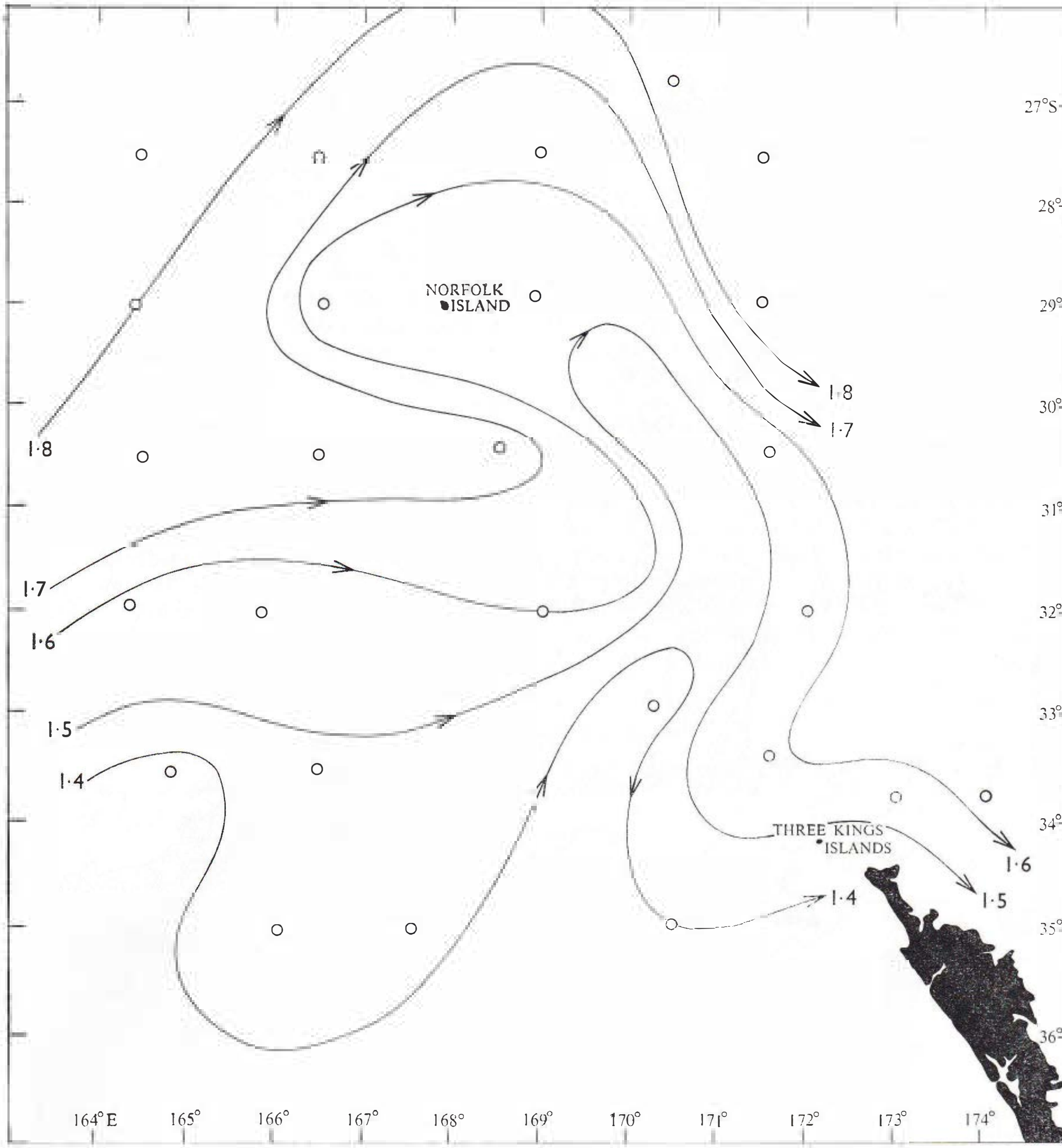

FIG. 2. Geopotential topography of the sea surface relative to the 1,000 decibar isobaric surface. Contours of geopotential anomaly are in dynamic metres and are also stream-lines of the relative geostrophic flow at the surface, in the direction of the arrows.

Current an extensive, weaker flow towards the west or south-west between 10° S and 30° S at the surface in the south-west Pacific, practically opposite to the flow indicated by the geopotential topography. Wyrtki (1962b) stated that "this flow to the west, the Trade Drift, is a wind drift at the surface, and consequently cannot appear as a geostrophic current". Since other major wind-driven currents seem to be associated with rather deep-lying horizontal pressure gradients arising from the mutual adjustment of velocity and density (for example, the South Equatorial and Circumpolar Currents), this implies the existence of a rather special, almost completely ageostrophic, situation. Reid (1961), also, compares various current atlases with the general surface topography

This work is licensed under the Creative Commons Attribution-NonCommercial-NoDerivs 3.0 Unported License.
To view a copy of this license, visit http://creativecommons.org/licenses/by-nc-nd/3.0/

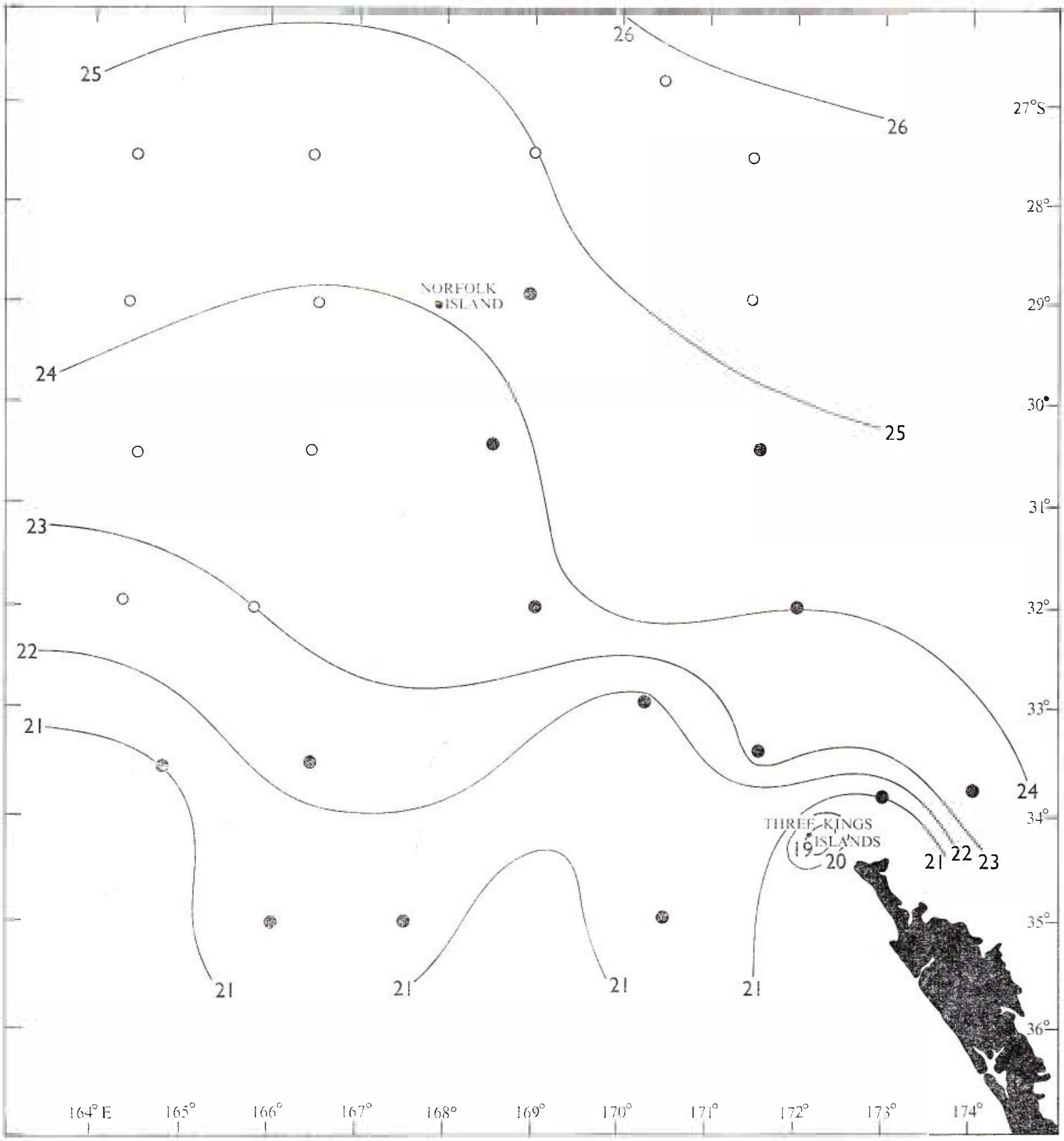

FIG. 3. Isotherms of sea surface temperature (°C) derived from station data and thermograph records along the cruise track. Filled circles at the station positions mark the absence of a well defined isothermal upper mixed layer.

of the whole Pacific Ocean relative to the 1,000 decibar surface. He concluded, through the good general agreement, that "the geostrophic currents can be accepted with some confidence in areas where other data are lacking". From experience with the magnitude of the ship's leeway while hove-to on station during the current survey series, one wonders whether these "current charts" derived from navigational records can do other than measure some effect of mean wind patterns, except in regions of rather strong, steady currents. Reid (1961) pointed out that "where current and wind are opposed geopotential anomaly will decrease along a streamline", and vice versa, thus accounting for a rise in dynamic topography towards the west in the trade-wind region.

This work is licensed under the Creative Commons Attribution-NonCommercial-NoDerivs 3.0 Unported License.
To view a copy of this license, visit http://creativecommons.org/licenses/by-nc-nd/3.0/

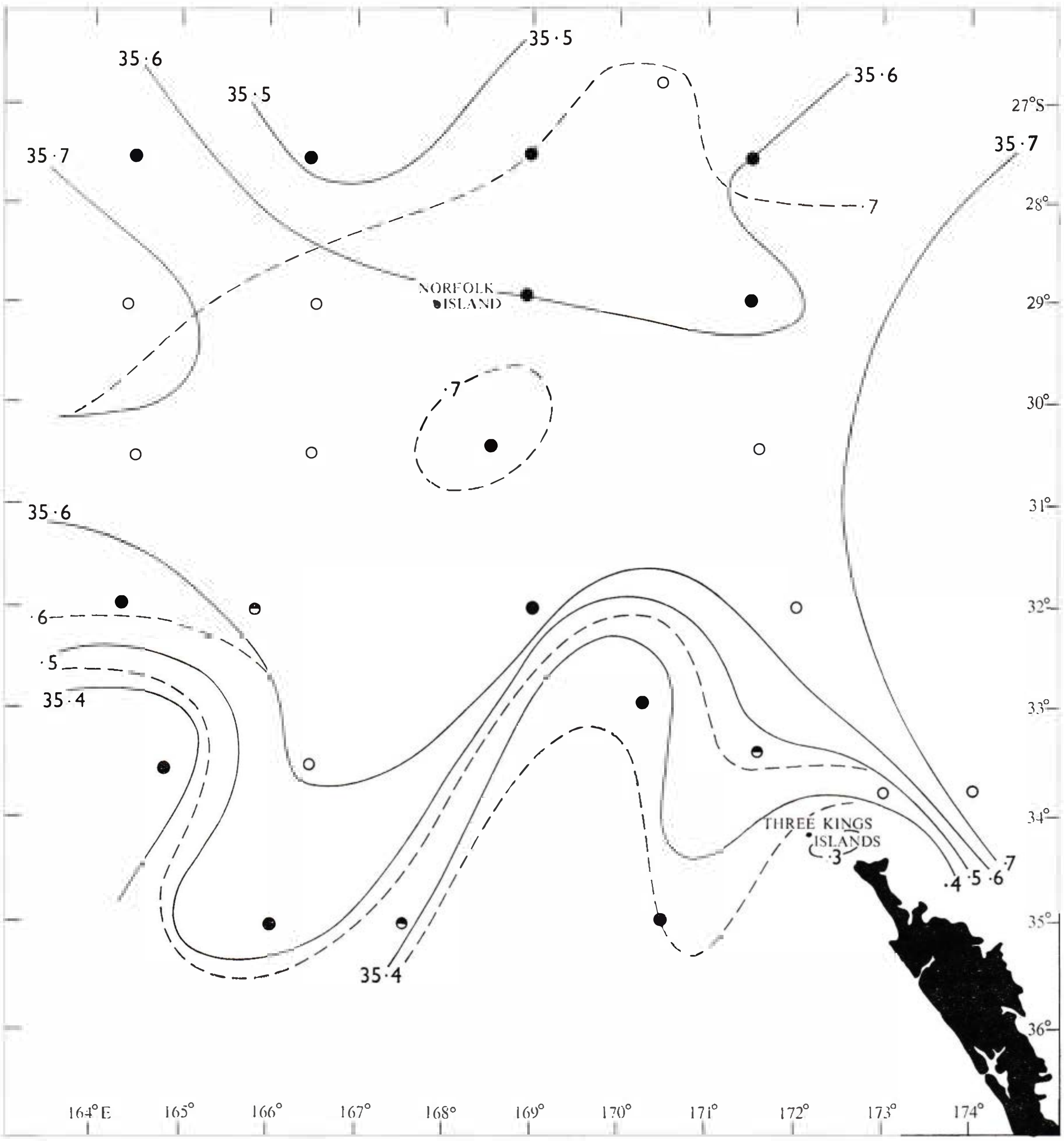

FIG. 4. Full lines are isohalines of the sea surface salinity (‰). Broken lines are isohalines on the surface of maximum salinity. Where these converge the salinity maximum lies at the surface. Filled circles at the station positions mark the existence of a subsurface maximum in the salinity-depth measurements.

SURFACE TEMPERATURE AND SALINITY

Surface temperature over the survey area (Fig. 3) ranged from nearly 26°c in the north-east to about 21°c in the south. A localised area of lower surface temperature (~ 19°c) between the Three Kings Islands and the northern coast of New Zealand presumably marked upwelling on the shelf. This region was traversed at night in very calm conditions, and the cooler surface waters contained large numbers of phosphorescent animals. Surface isotherms over the survey area had a marked trend from the north-west to the south-east, surface water being considerably warmer in the east of the area than in the west.

This work is licensed under the Creative Commons Attribution-NonCommercial-NoDerivs 3.0 Unported License.
To view a copy of this license, visit http://creativecommons.org/licenses/by-nc-nd/3.0/

A broad ridge of high salinity (~35.7‰) with its axis following, approximately, the trend of the 24°C isotherm dominated the surface salinity distribution (Fig. 4). Both surface temperature and salinity decreased fairly rapidly to the south of this ridge. Isolines had a wave-like configuration with warm, highly saline water tending to lie over the bottom ridges and colder, less saline water over the troughs. For the basically east-going flow through the survey area described in the previous section, these deflections accord with elementary theories concerning the influence of bottom topography on ocean currents described, for example, by Defant (1961, pp. 429–36).

Simple correlation between surface temperature and salinity was no longer evident on the northern side of the high salinity ridge, where isotherms and isohalines tended to intersect at large angles. Lowest salinity in this region was found north-west of Norfolk Island, and highest surface temperature was found in the north-east of the survey area.

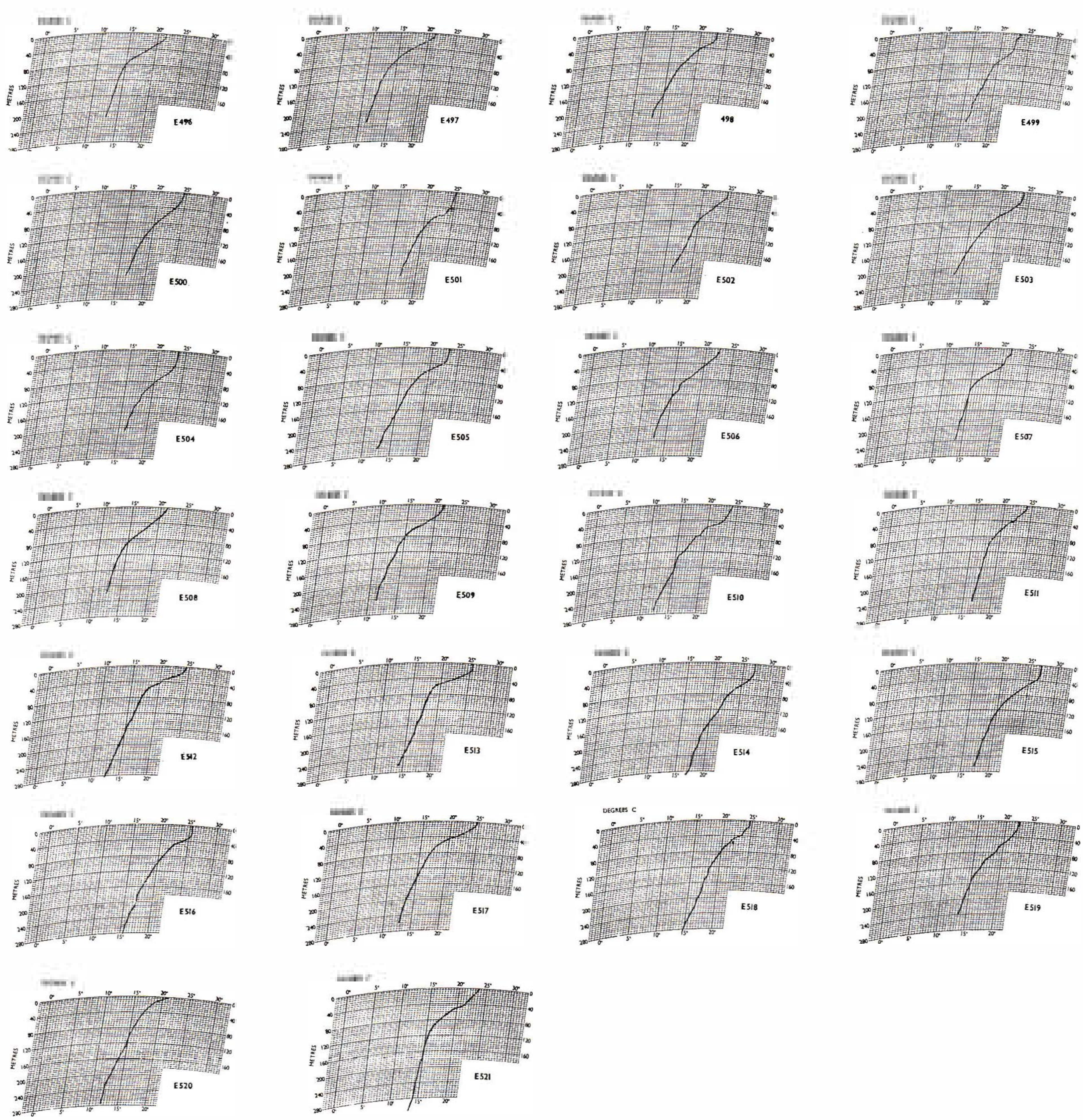

FIG. 5. Bathythermograph traces from the stations indicated.

Inset 2*

This work is licensed under the Creative Commons Attribution-NonCommercial-NoDerivs 3.0 Unported License.
To view a copy of this license, visit http://creativecommons.org/licenses/by-nc-nd/3.0/

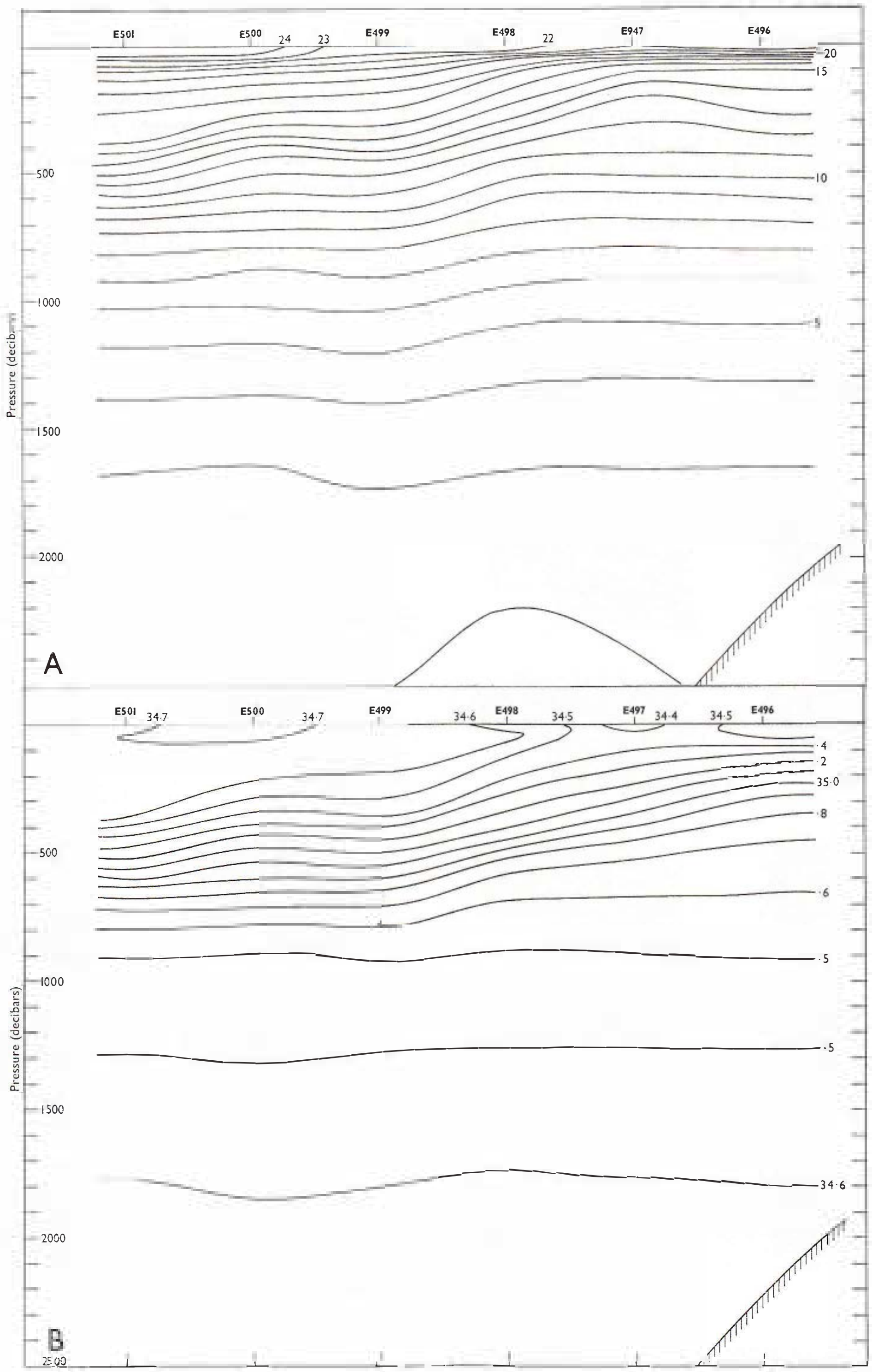

FIG. 6A. Vertical cross section of temperature, °C, along the western side of the New Caledonia Basin.
B. Vertical cross section of salinity, ‰, along the western side of the New Caledonia Basin.
North is at the left. The scale of pressure is numerically close to that of depth in metres (see Appendix).

This work is licensed under the Creative Commons Attribution-NonCommercial-NoDerivs 3.0 Unported License.
To view a copy of this license, visit http://creativecommons.org/licenses/by-nc-nd/3.0/

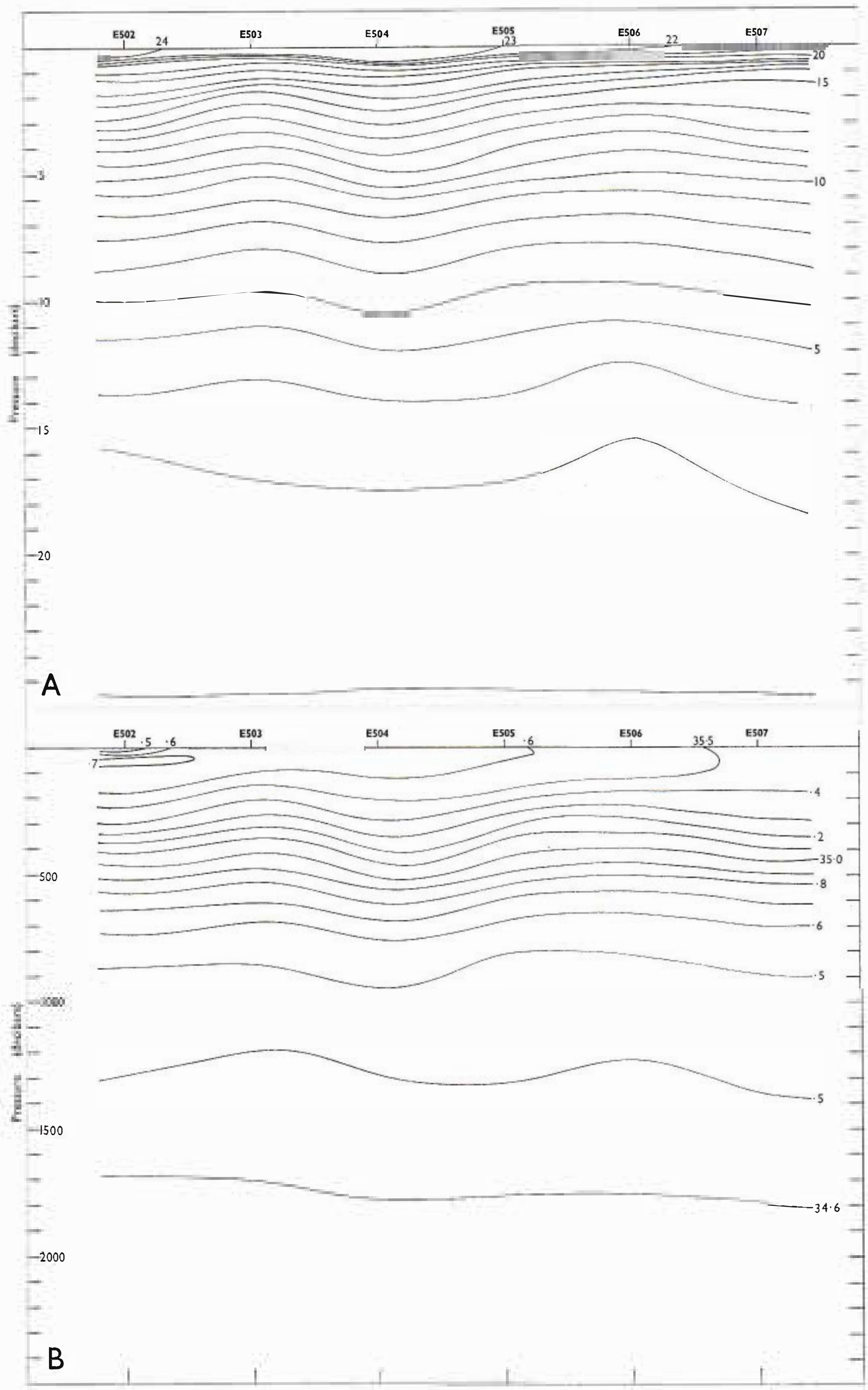

FIG. 7A. Vertical cross section of temperature, °C, along the eastern side of the New Caledonia Basin.
B. Vertical cross section of salinity, ‰, along the eastern side of the New Caledonia Basin.
North is at the left. The scale of pressure is numerically close to that of depth in metres (see Appendix).

This work is licensed under the Creative Commons Attribution-NonCommercial-NoDerivs 3.0 Unported License.
To view a copy of this license, visit http://creativecommons.org/licenses/by-nc-nd/3.0/

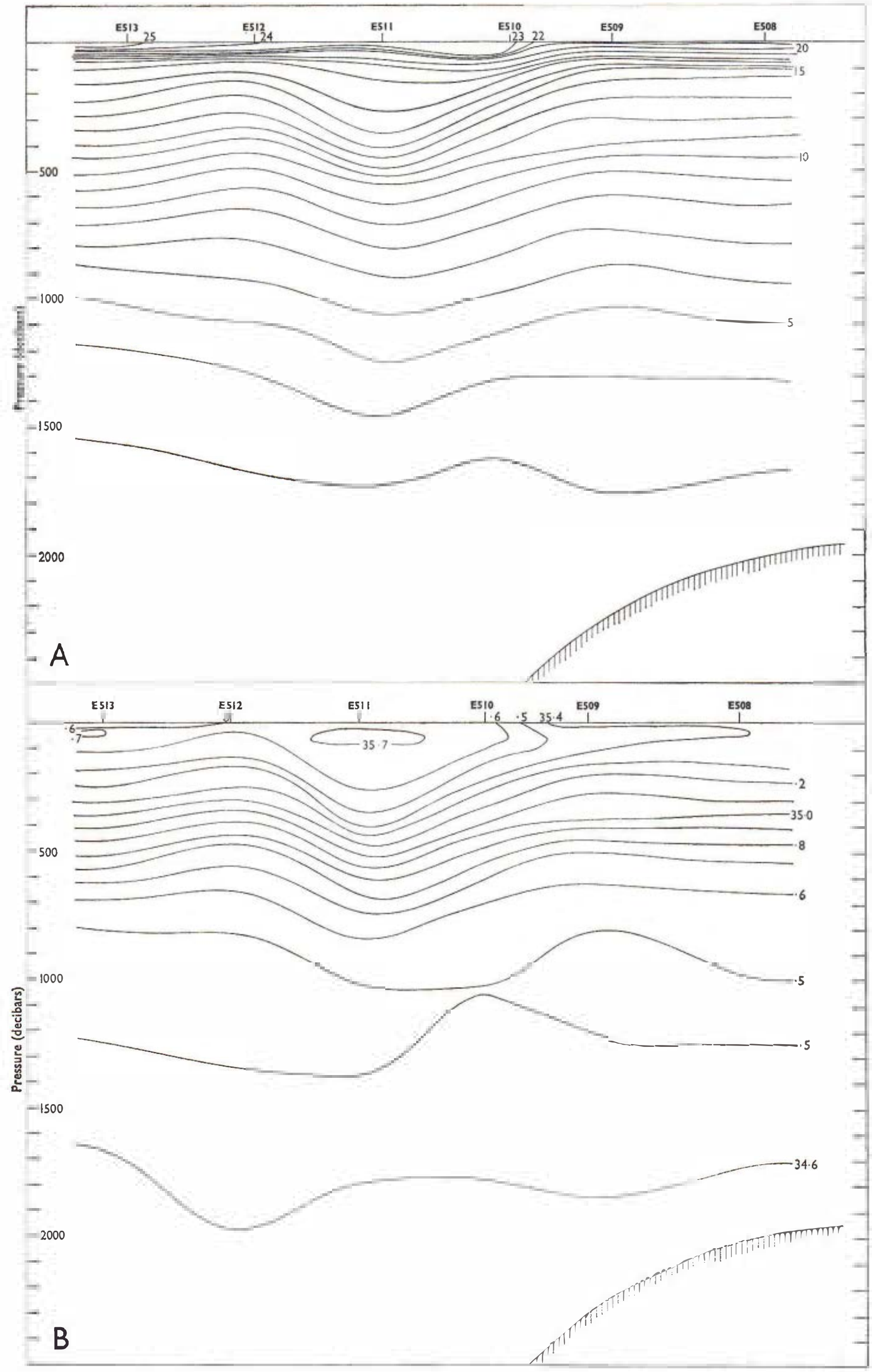

FIG. 8 A. Vertical cross section of temperature, °C, along the eastern side of the Norfolk Ridge. B. Vertical cross section of salinity, ‰, along the eastern side of the Norfolk Ridge. North is at the left. The scale of pressure is numerically close to that of depth in metres (see Appendix).

This work is licensed under the Creative Commons Attribution-NonCommercial-NoDerivs 3.0 Unported License.
To view a copy of this license, visit http://creativecommons.org/licenses/by-nc-nd/3.0/

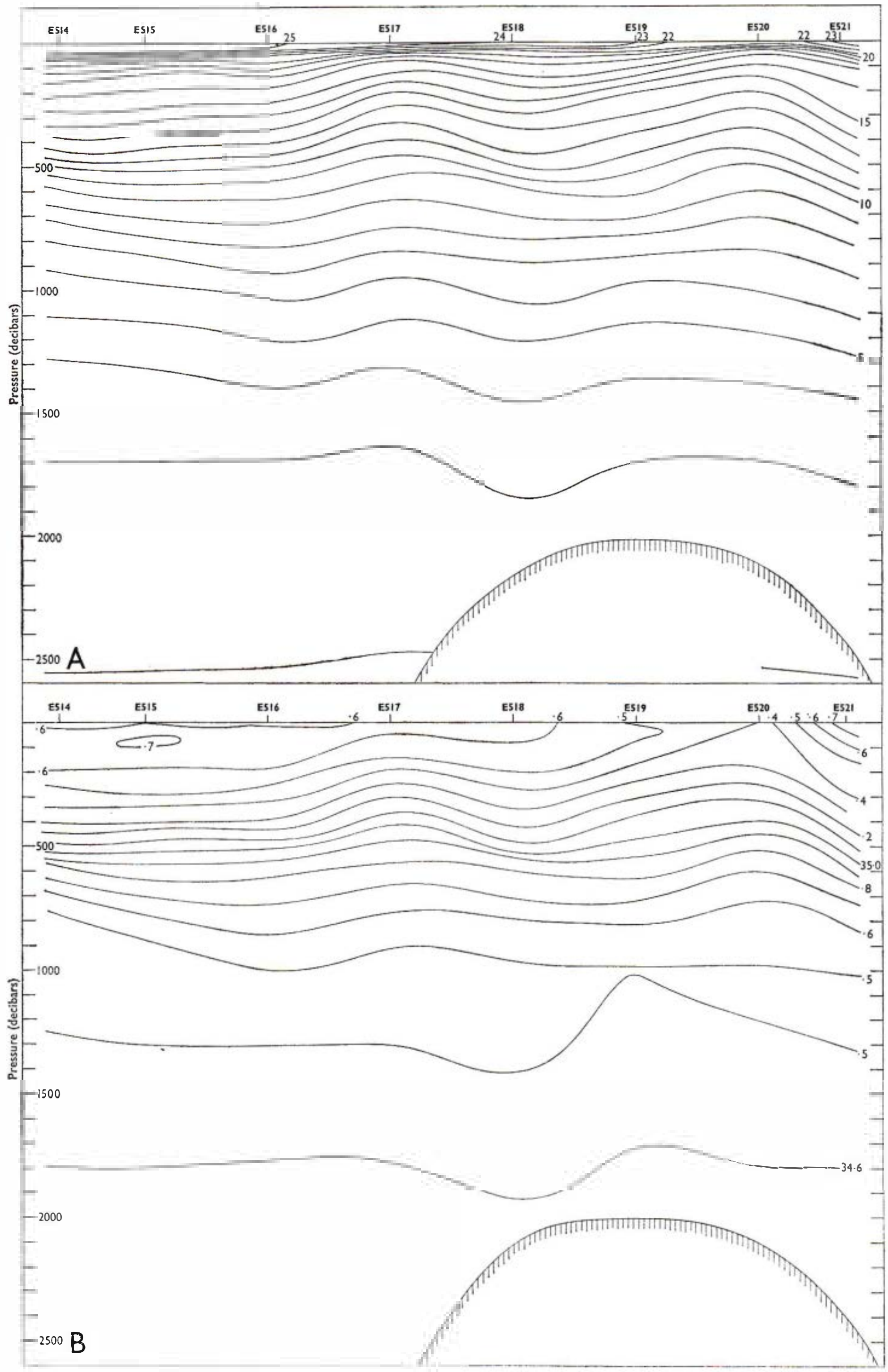

FIG. 9A. Vertical cross section of temperature, °C, to the north of New Zealand.
B. Vertical cross section of salinity, ‰, to the north of New Zealand.
North is at the left. The scale of pressure is numerically close to that of depth in metres (see Appendix).

This work is licensed under the Creative Commons Attribution-NonCommercial-NoDerivs 3.0 Unported License.
To view a copy of this license, visit http://creativecommons.org/licenses/by-nc-nd/3.0/

SUBSURFACE PROPERTIES

Upper Mixed Layer

At some stations of the survey the top of the thermocline layer was at a depth of several tens of metres and was overlain by a nearly isothermal upper mixed layer. At other stations the temperature decreased steadily with increasing depth right from the sea surface. A clearly defined example of the first situation may be seen in the bathythermograph trace from Sta. E 515 (Fig. 5), where the upper isothermal layer was about 36 m thick, and the transition at its base to the upper part of the thermocline layer was particularly pronounced. An extreme example of the second situation was found at Sta. E 508 where the bathythermograph trace (Fig. 5) revealed a nearly constant vertical temperature gradient from a depth of some 80 m right up to the sea surface. Not all the bathythermograms obtained can be readily placed in these two classes, but there was a tendency for soundings of the second kind, in which the upper mixed layer was absent or ill defined, to occur along the southern side of the region of high surface salinity, and in the topographic trough (below the 1.6 dynamic metre contour, say) which extended into this region. This division can also be seen in the vertical temperature cross sections, especially south of Sta. E 498 (Fig. 6A) and south of E 510 (Fig. 8A).

Bathythermograph traces obtained during an earlier survey of this series (Garner, 1967b) show that the isothermal upper mixed layer had recovered its structure in the northern part of the south-east Tasman Sea (latitude 41–42° S) but had lost it again further to the south in the region of the Subtropical Convergence. Possibly, these variations in the thermal structure of near-surface waters with latitude are due to corresponding variations of vertical velocity components associated with zones of horizontal convergence and divergence in the surface ocean circulation. The absence of an isothermal upper mixed layer would then be due to a continued upwards movement of colder water into near-surface layers at a rate sufficient to counteract the effect of vertical mixing by wind and wave.

The upper 200 m or so of the water column is, in general, a region of rather weak vertical salinity gradient. The top of the halocline layer, in which the salinity begins to fall rather rapidly with increasing depth, is particularly well marked in the vertical cross sections of Figs. 6B and 8B. Where this halocline lies deepest an inflexion is also present in the temperature depth curve at the top of the halocline (for example, at about 350 m at Sta. E 501, and about 250 m at Sta. E 511). This is similar to the situation typical of many stations in the south-east Tasman Sea (Garner, 1967b) for which it was suggested that the upper nearly isohaline region represents the upper mixed layer in its maximum winter development. If this explanation is valid, at the two stations mentioned above the summer thermocline layer in the upper 100 m of the water column can be distinguished from the top of the permanent thermocline at the greater depth.

Salinity Maximum

At all stations within the region of high surface salinity (>35.7‰, say) except for sta. E 511, salinity decreased steadily with increasing depth throughout the upper part of the water column. Beneath the surface water of lower salinity found in both northern and southern parts of the survey area, however, salinity increased with depth to reach a weak maximum between 30 and 100 m. Except for an isolated high around Sta. E 511, salinity on the surface of maximum salinity increased northwards over the whole survey area, as shown by the broken isohalines in Fig. 4. Large-scale maps of the surface oceanic salinity distribution (for example, Defant, 1961, Plate 5) show that the source of high salinity water in the South Pacific is centred in the eastern subtropical part of this ocean (at about 20° S, 120° W). From this centre a ridge of high salinity extends westwards past the north of New Zealand almost to the east coast of Australia. From comparison of the topography and salinity patterns of Figs. 1 and 4, it would appear that the high salinity water north of New Zealand found during the present investigation was flowing eastwards out from the Tasman Sea, having presumably been introduced into the Coral Sea at some lower latitude from the subtropical source region. Comparison of the salinity distribution in upper water layers with Wyrtki's (1962a) classification of water masses in the south-west Pacific region, however, identifies this high salinity water with the southern component of his *subtropical lower water* which, he suggests, enters the Coral Sea to the north of New Zealand, and is continuous with the subtropical surface water of the eastern Pacific. The zonal salinity gradient along the axis of the high surface salinity ridge in Fig. 4 is indeterminate, but Wyrtki's geographically more extensive study showed salinity in the core of the southern component of the subtropical lower water to be increasing eastwards, indicating the spreading of this water from that direction, either by direct flow or by lateral mixing.

This work is licensed under the Creative Commons Attribution-NonCommercial-NoDerivs 3.0 Unported License.
To view a copy of this license, visit http://creativecommons.org/licenses/by-nc-nd/3.0/

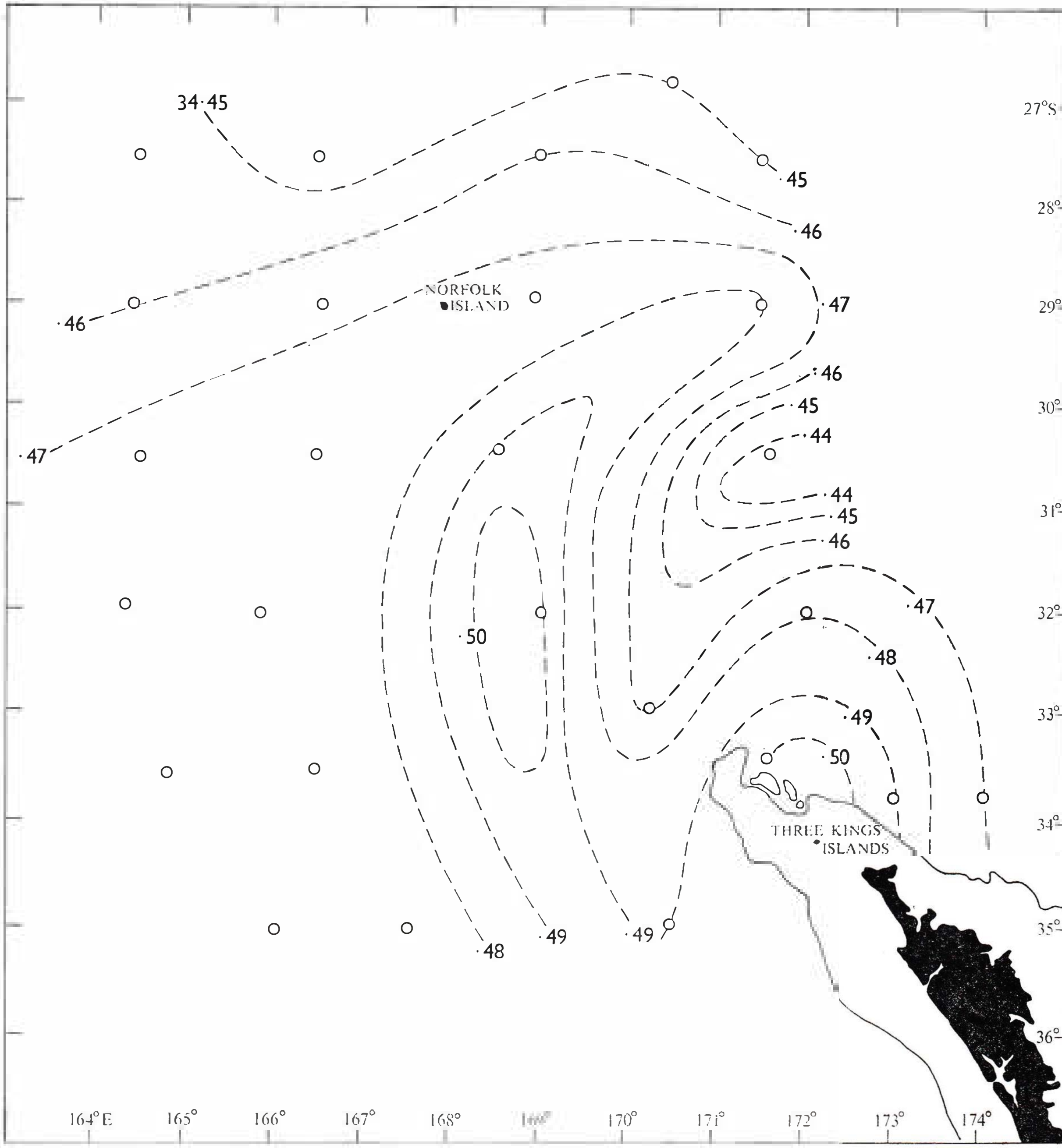

FIG. 10. Isohalines (‰) of salinity in the core of the Antarctic Intermediate Water. The position of the 1 km isobath around the north of New Zealand is indicated.

Resolution of the direction of movement of subtropical water to the north of New Zealand will probably require direct measurement of current flow, independent of the hydrology.

Wyrtki's (1962a) analysis was based on observations made during the late summer of 1960, and revealed salinities in the subtropical water north of New Zealand rather higher (<35.9‰) than were found by this survey (~ 35.7‰). Salinity greater than 35.9‰ was also encountered around the northern part of New Zealand in the summer of 1955 (Garner, 1961, Fig. 3), and again in summer, 1967 (Garner and Ridgway, 1965, Fig. 45), so the influence of this water mass may not have been as pronounced during the survey period as it can sometimes appear to be.

Inset 3

This work is licensed under the Creative Commons Attribution-NonCommercial-NoDerivs 3.0 Unported License.
To view a copy of this license, visit http://creativecommons.org/licenses/by-nc-nd/3.0/

Wyrtki (1960) states than monsoon winds bring relatively low-salinity equatorial waters from the western Pacific into the Coral Sea during January-March. The lower surface salinities in the northern part of the survey area will thus represent the southern limit of the incursion of this equatorial water. During September 1966 it was found (B. R. Stanton, pers. comm.) that surface salinity continued to rise slowly between the northern part of the survey area and New Caledonia, where a value of about 35.8‰ was reached.

The mean current charts referred to earlier show a *Tropical Convergence* to the north of New Zealand where the Trade Drift, moving south-westwards, meets the east-flowing water from the Tasman Sea circulation system around the north of North Island. The maps of Wyrtki (1960) show the seasonal movement in latitude of this feature; it appears furthest south, around 30° S, during the summer months but loses its definition in February. From the above definition it might be expected that the Tropical Convergence would be marked by the southern edge of the belt of high surface salinity—by the more southerly 35.6‰ isohaline in Fig. 4, for instance. In comparing the hydrology with the mean current maps, however, Wyrtki (1962) stated that the position of the Tropical Convergence coincided with the *northern* boundary of the southern component of the subtropical lower water north of New Zealand; south of the Convergence the salinity maximum was said to lie at the surface, while to the north a subsurface maximum was described. No hydrological structure suggesting the existence of a tropical convergence was revealed by the present survey.

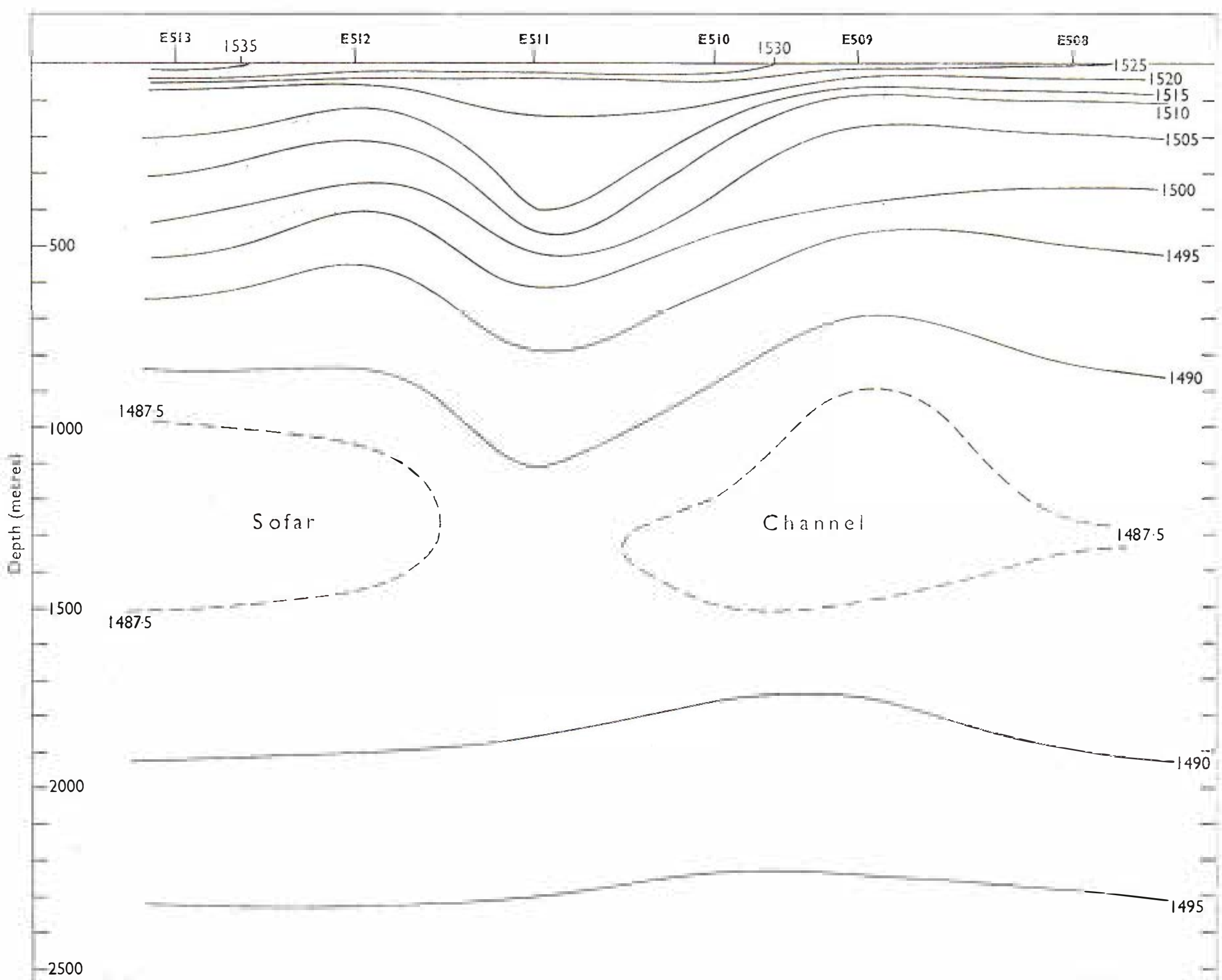

FIG. 11. Vertical cross section of sound velocity (m/sec) along the eastern side of the Norfolk Ridge, corresponding to the hydrological sections of Fig. 8.

This work is licensed under the Creative Commons Attribution-NonCommercial-NoDerivs 3.0 Unported License.
To view a copy of this license, visit http://creativecommons.org/licenses/by-nc-nd/3.0/

Antarctic Intermediate Water

Below the halocline, salinity decreased with increasing depth at all stations to reach a minimum (<34.5‰) at about 1.1 km. This minimum marks the core of the Antarctic Intermediate Water the properties of which, over the Pacific as a whole, have been discussed by Reid (1965) and, for the south-west Pacific in particular, by Wyrtki (1962a). Both these studies show that the Antarctic Intermediate Water enters the Coral Sea from the east between Fiji and New Zealand. Wyrtki (1962a, Fig. 12) found a tongue of low salinity (<34.4‰) in the Intermediate core between latitudes 22° S and 27° S south of Fiji, extending westwards towards New Caledonia. He suggested that this branch was derived from a strong northward flow of Antarctic Intermediate Water around the end of the Chatham Rise east of New Zealand. Reid (1965, Fig. 24), looking at a geographically more extensive situation, described a similar tongue south of Fiji but showed that its origin extended well into the eastern Pacific. It was inferred that the Antarctic Intermediate Water reached the Coral Sea by way of a long gyral involving, in turn, the deeper waters of the Circumpolar, the Peru, and the South Equatorial Currents.

The variation of salinity on the minimum surface throughout the survey area has been plotted (Fig. 10). Salinity gradients on this surface were very weak, as is general over the whole Tasman Sea. A tendency is evident for slightly higher salinities (~34.5‰) to lie over the shallower water north of the Three Kings Islands (Sta. E 519) and the southern part of the Norfolk Ridge (Sta.E 510). This effect, presumably due to increased vertical mixing over topographic features, has been noticed elsewhere for the Antarctic Intermediate layer (Garner, 1967b). Salinity on the minimum surface fell in the north and north-eastern parts of the survey area. This trend is associated with the presence to the near north of the main inflow of Antarctic Intermediate Water into this region, as described earlier.

Deep Water

Below the core of the Antarctic Intermediate Water salinity increased slowly with increasing depth. The stations of this survey were designed to reach a depth of 2–2.5 km, sufficient to define adequately the Intermediate salinity minimum but not necessarily to sample the deepest waters of the basins investigated. Deep data are sufficient, however, to show that a greater vertical salinity gradient was observed below the Intermediate core in the south-east Tasman Sea (Garner, 1967b, Fig. 5) (giving a salinity around 34.7‰ at a depth of 2 km) than in the present work for the New Caledonia Trough (Figs. 6B and 7B) (where deep salinity was just over 34.6‰ in water of equivalent temperature).

These differences are explained by Wyrtki (1961), who found that the deeps of the New Caledonia Trough and the South Fiji Basin are filled, from the north, with Pacific Bottom Water—a derivative of the Antarctic Bottom Water. This water also fills the bottom of the Tasman Basin but, unlike areas further north, it has a weak salinity maximum at a depth of about 3 km in the Tasman. This marks the core of the Pacific Deep Water, a remnant of North Atlantic Deep Water, the presence of which accounts for the higher salinity of the deeper waters in the Tasman Basin, south of the Lord Howe Rise.

SOUND VELOCITY

This survey provides a further contribution towards definition of the SOFAR sound channel configuration around New Zealand. Apart from some very small fluctuations in the upper mixed layer at a few stations, sound velocity decreased with increasing depth over the survey area to reach a minimum at some 1,300 m. This minimum marks the axis of the SOFAR sound channel, the general characteristics of which have been described for the New Zealand region by Garner (1967c). A vertical cross section of sound velocity along the eastern side of the Norfolk Ridge (Fig. 11) matches the hydrological sections of Fig. 8. The velocity of sound in the SOFAR axis of this section reached a maximum of nearly 1,490 m/sec at Sta. E 511. Comparison of Figs. 8 and 11 shows that this was derived from the dip in all isopleths at this station associated with the large wave in the generally east-going geostrophic flow east of the Norfolk Ridge. A sound velocity maximum in the SOFAR axis also appeared in the other meridional sections (not reproduced here) corresponding to Figs. 6, 7, and 9, but more weakly defined than was shown in Fig. 11. A belt of high SOFAR velocity thus appeared to run zonally through the centre of the survey area, its axis defined by Sta. E 499, E 504, E 511, and E 518, in about latitude 31° S. The earlier general study of SOFAR channel characteristics (Garner, 1967c), based on a compilation of hydrological stations in the New Zealand region, also showed that "this belt of high sound velocity extends north-westwards from the northern tip of New Zealand, passing between Norfolk and Lord Howe Islands". It was suggested that the isotherm dip associated with

Inset 3*

This work is licensed under the Creative Commons Attribution-NonCommercial-NoDerivs 3.0 Unported License.
To view a copy of this license, visit http://creativecommons.org/licenses/by-nc-nd/3.0/

this belt would probably mark the dynamical boundary "between a general west-going movement of water into the Tasman Sea to the north of 30° S, and an east-going flow out from the Tasman between this latitude and New Zealand". This interpretation would imply the existence north of 30° S of a west-flowing movement more general than was indicated by the present survey, which revealed, rather, a localised flow with a west-going component due to perturbation of an east-flowing stream.

Echo-sounding Corrections

A further contribution, too, is made to a re-evaluation for the New Zealand region of Matthews' (1939) tables for the correction of sonic soundings in terms of regional variations of the velocity of sound. Table 2 gives a comparison of mean vertical sounding velocities, and corrections to an echo-sounding machine calibrated for a velocity of 1,500 m/sec, between Matthews' estimates for the survey area (his region 46) and the survey data. This is given for a northern station, E 515, and for a southern station, E 507. Observed values for the southern station are closely approximated by Matthews' estimates. In the north of the survey area the corrections derived tend to be rather larger than those given in the earlier tables.

TABLE 2. Sounding Velocities and Corrections

Column A—depth (metres).

Column B—mean vertical sounding velocity (m/sec).

Column C—correction (metres) to be applied algebraically to the sounding from a machine set for a velocity of 1,500 m/sec.

	Matthews area 46		Station E 507		Station E 514	
A	B	C	B	C	B	C
2	1524	3	1514.5	1.9	1526.4	3.5
4	1517	4	1510.3	2.8	1521.0	5.7
6	1510	4	1506.8	2.6	1516.1	6.5
8	1505	3	1503.3	1.8	1511.5	6.1
10	1501	1	1500.9	0.6	1507.4	4.8
12	1499	− 1	1498.9	−0.9	1504.0	3.3
14	1497	− 3	1497.4	−2.6	1501.7	1.6
16	1496	− 4	1496.1	−4.1	1499.5	−0.1
18	1495	− 6	1495.5	−5.5	1498.4	−1.5
20	1495	− 7	1495.4	−6.6	1498.0	−2.6
22	1494	− 9	1495.2	−7.4	1497.7	−3.4
24	1494	−10	1495.0	−8.0	1497.5	−4.0
26	1495	− 9	1495.0	−8.5	1497.2	−4.5

ACKNOWLEDGMENTS

Station overside work was done by A. Langford, W. Main, and I. Slater, NZOI, and M. Johnstone, University of Queensland. N. M. Ridgway made salinity determinations and checked all thermometer readings. The writer is grateful for the assistance of this team and for the ready co-operation of Captain D. K. Matheson and his crew.

This work is licensed under the Creative Commons Attribution-NonCommercial-NoDerivs 3.0 Unported License.
To view a copy of this license, visit http://creativecommons.org/licenses/by-nc-nd/3.0/

REFERENCES

BARK, L. S.; GANSON, P. P.; MEISTER, N. A. 1964: "Tables of the Velocity of Sound in Sea Water". Pergamon Press, London.

DEFANT, A. 1961: "Physical Oceanography Vol. I". Pergamon Press, London. 729 pp.

GARNER, D. M. 1961: Hydrology of New Zealand Coastal Waters, 1955. *Bull. N.Z. Dep. scient. ind. Res. 138.*

—— 1967a: Hydrology of the Southern Hikurangi Trench Region. *Bull. N.Z. Dep. scient. ind. Res. 177.*

—— 1967b: Hydrology of the South-east Tasman Sea. *Bull. N.Z. Dep. scient. ind. Res. 181.*

—— 1967c: Oceanic Sound Channels around New Zealand. *N.Z. Jl mar. Freshwat. Res. 1* (*1*): 3–15.

GARNER, D. M.; RIDGWAY, N. M. 1965: Hydrology of New Zealand Offshore Waters. *Bull. N.Z. Dep. scient. ind. Res. 162.*

LAFOND, E. C. 1951: Processing Oceanographic Data. *Publs U.S. hydrogr. Off. 614.*

MATTHEWS, D. J. 1939: Tables of the Velocity of Sound in Pure Water and Sea Water for Use in Echo-sounding and Sound Ranging. *Publs Admiralty hydrogr. Dep. 282.*

REID, J. L. 1961: On the Geostrophic Flow at the Surface of the Pacific Ocean with respect to the 1,000 decibar Surface. *Tellus 13* (*4*): 489–502.

—— 1965: Intermediate Depth Waters of the Pacific Ocean. *Johns Hopkins Univ. Stud. Oceanogr. 2.*

RIDGWAY, N. M. (in press): Hydrology of the Southern Kermadec Trench Region. *Bull. N.Z. Dep. scient. ind. Res. 56.*

UNITED STATES NAVY HYDROGRAPHIC OFFICE, 1956: Tables for Rapid Computation of Density and Electrical Conductivity of Sea Water. *Publs U.S. hydrogr. Off. SP-11.*

WYRTKI, K. 1960: The Surface Circulation in the Coral and Tasman Seas. *Tech. Pap. Div. Fish. Oceanogr. C.S.I.R.O. Aust. 8.*

—— 1961: The Flow of Water into the Deep Basins of the Western South Pacific Ocean. *Aust. J. mar. Freshwat. Res. 12*: 1–16.

—— 1962a: The Subsurface Water Masses in the Western South Pacific Ocean. *Ibid. 13* (*1*): 18–47.

—— 1962b: Geopotential Topographies and Associated Circulation in the Western South Pacific Ocean. *Ibid. 13* (*2*): 89–105.

This work is licensed under the Creative Commons Attribution-NonCommercial-NoDerivs 3.0 Unported License.
To view a copy of this license, visit http://creativecommons.org/licenses/by-nc-nd/3.0/

APPENDIX

Numerical Station Data

Station numbers are prefixed with the letter E. Positions, dates, etc., of stations are listed in Table 1. The significance of column headings is as follows:

P is the thermometrically measured pressure in decibars at each sampling point. This is numerically nearly equal to the geometric depth in metres. A more accurate conversion using representative mean density figures (LaFond, 1951, p. 8) is as follows:

pressure (*decibars*):	200	400	600	800	1000	1500	2000	2500
depth (*metres*):	199	398	595	793	991	1484	1976	2467

T is the water temperature in °C.

S is the water salinity in ‰.

σ_t is the water density, isothermally reduced to surface pressure. The "σ" value is derived from the specific gravity, ρ, according to the relation:

$$\sigma = (\rho - 1) \times 10^5$$

$\Sigma\Delta D$ is the cumulative anomaly of dynamic height (LaFond, 1951) of the sea surface from the sample depth. Expressed in dynamic metres.

C is the *in situ* sound velocity (Bark *et al.*, 1964) in m/sec.

This work is licensed under the Creative Commons Attribution-NonCommercial-NoDerivs 3.0 Unported License.
To view a copy of this license, visit http://creativecommons.org/licenses/by-nc-nd/3.0/

E496

P	T	S	σ_t	ΣΔD	C
0	21.43	35.53	24.81	0.00	1526.3
9	21.34	35.53	24.83	0.03	1526.2
18	21.16	35.55	24.90	0.06	1525.9
27	19.95	35.55	25.23	0.08	1522.7
45	18.67	35.54	25.54	0.13	1519.3
63	16.44	35.46	26.03	0.17	1513.0
98	15.20	35.33	26.21	0.24	1509.5
137	14.41	35.24	26.31	0.31	1507.4
178	13.93	35.19	26.38	0.38	1506.4
273	13.09	35.10	26.48	0.54	1505.0
352	12.12	34.99	26.59	0.66	1502.9
446	10.83	34.85	26.71	0.80	1499.8
542	9.75	34.74	26.82	0.94	1497.2
656	8.12	34.60	26.97	1.08	1492.9
711	7.53	34.56	27.02	1.15	1491.5
789	6.89	34.52	27.09	1.24	1490.2
885	6.20	34.48	27.14	1.34	1489.0
989	5.68	34.48	27.21	1.45	1488.6
1043	5.32	34.48	27.25	1.51	1487.9
1314	3.94	34.51	27.44	1.74	1486.8
1794	2.73	34.60	27.62	2.07	1489.5
2248	2.26	34.65	27.70	2.32	1494.9

E497

P	T	S	σ_t	ΣΔD	C
0	20.98	35.33	24.77	0.00	1525.0
5	20.94	35.33	24.78	0.02	1525.0
10	20.84	35.33	24.81	0.03	1524.7
15	20.40	35.39	24.97	0.05	1523.6
25	19.10	35.43	25.34	0.08	1520.2
38	18.05	35.48	25.65	0.11	1517.4
54	17.60	35.46	25.74	0.15	1516.4
72	16.91	35.44	25.89	0.18	1514.5
88	16.00	35.40	26.08	0.22	1511.9
133	14.15	35.35	26.44	0.30	1506.6
178	13.59	35.30	26.52	0.37	1505.4
210	13.07	35.24	26.58	0.42	1504.2
241	12.63	35.16	26.60	0.47	1503.2

E498

P	T	S	σ_t	ΣΔD	C
0	22.80	35.53	24.42	0.00	1529.9
7	22.74	35.52	24.43	0.02	1529.9
16	22.69	35.53	24.46	0.06	1530.0
24	21.72	35.53	24.73	0.08	1527.6
39	20.00	35.63	25.26	0.13	1523.1
54	19.08	35.62	25.49	0.17	1520.9
88	17.97	35.57	25.74	0.25	1518.1
163	16.12	35.48	26.12	0.41	1513.5
238	14.41	35.35	26.39	0.58	1509.4
326	13.33	35.25	26.55	0.69	1506.8
413	11.60	35.09	26.66	0.83	1502.2
504	10.28	34.84	26.70	0.96	1498.9
580	9.20	34.70	26.78	1.07	1495.8
675	8.06	34.61	26.97	1.19	1492.9
760	7.47	34.56	27.03	1.29	1492.1
839	6.94	34.52	27.08	1.38	1491.2
930	6.12	34.48	27.15	1.48	1489.4
988	5.65	34.47	27.20	1.54	1488.4
1225	4.42	34.49	27.37	1.75	1487.2
1642	3.05	34.58	27.57	2.03	1488.3
1879	2.52	34.62	27.65	2.18	1490.0

E499

P	T	S	σ_t	ΣΔD	C
0	23.32	35.68	24.39	0.00	1531.5
19	23.06	35.68	24.46	0.07	1531.1
24	23.06	35.68	24.46	0.08	1531.2
32	23.03	35.68	24.47	0.11	1531.1
68	22.29	35.66	24.67	0.23	1529.9
75	20.28	35.65	25.20	0.26	1524.5
101	19.56	35.65	25.40	0.33	1522.8
151	18.50	35.61	25.65	0.45	1520.6
204	17.70	35.59	25.83	0.57	1519.2
302	16.26	35.49	26.10	0.78	1516.3
401	14.32	35.30	26.38	0.97	1511.4
498	12.33	35.09	26.62	1.13	1506.1
594	10.78	34.91	26.77	1.28	1502.1

E499 (con t'd)

P	T	S	σ_t	ΣΔD	C
701	9.16	34.71	26.89	1.42	1498.8
809	7.93	34.59	26.99	1.56	1494.7
902	7.04	34.51	27.06	1.67	1492.6
989	6.34	34.49	27.13	1.76	1491.2
1102	5.67	34.47	27.20	1.88	1490.7
1200	5.05	34.48	27.28	1.98	1490.6
1500	3.65	34.55	27.49	2.23	1488.5
2000	2.45	34.63	27.67	2.55	1491.7
2500	2.02	34.68	27.75	2.80	1498.1

E500

P	T	S	σ_t	ΣΔD	C
0	24.54	35.74	23.16	0.00	1534.5
10	24.35	35.74	24.13	0.04	1534.3
20	24.19	35.74	24.18	0.08	1534.0
30	23.85	35.74	24.28	0.12	1533.3
49	22.87	35.72	24.75	0.18	1531.2
69	21.52	35.68	24.89	0.25	1527.9
98	20.20	35.66	25.24	0.33	1524.8
147	19.29	35.63	25.46	0.46	1522.9
188	18.35	35.61	25.68	0.56	1520.8
277	16.82	35.50	25.97	0.76	1517.5
365	14.76	35.33	26.30	0.94	1512.3
471	12.49	35.09	26.59	1.12	1506.3
564	11.21	34.96	26.73	1.26	1503.2
654	9.97	34.80	26.83	1.39	1500.1
755	8.44	34.63	26.95	1.52	1495.8
842	7.18	34.52	27.04	1.62	1492.2
940	6.59	34.49	27.10	1.74	1491.5
1063	5.79	34.46	27.18	1.87	1490.2
1134	5.18	34.47	27.27	1.94	1489.0
1441	3.57	34.53	27.48	2.19	1487.1
1911	2.65	34.61	27.64	2.50	1491.1
2380	2.25	34.66	27.71	2.75	1497.1

E501

P	T	S	σ_t	ΣΔD	C
0	24.77	35.64	23.93	0.00	1535.0
9	24.68	35.64	23.95	0.04	1534.9
18	24.42	35.63	24.03	0.07	1534.4
28	24.20	35.62	24.08	0.11	1534.1
47	23.62	35.71	24.32	0.18	1532.9
74	21.98	35.66	24.78	0.27	1529.1
100	20.74	35.64	25.08	0.35	1526.2
150	19.49	35.64	25.41	0.49	1523.5
172	18.90	35.64	25.56	0.55	1522.1
270	17.86	35.64	25.81	0.78	1520.6
348	17.41	35.62	25.92	0.96	1520.6
434	15.62	35.39	26.16	1.14	1516.3
510	13.60	35.21	26.46	1.28	1510.7
598	11.70	35.00	26.67	1.42	1505.4
678	9.95	34.79	26.83	1.54	1500.3
751	8.70	34.65	26.92	1.64	1496.6
842	7.73	34.55	26.99	1.75	1494.4
944	6.87	34.48	27.06	1.87	1492.6
1001	6.25	34.46	27.12	1.93	1491.1
1248	4.56	34.49	27.35	2.18	1488.1
1683	2.93	34.58	27.58	2.50	1488.5
2103	2.47	34.64	27.68	2.75	1493.5

E502

P	T	S	σ_t	ΣΔD	C
0	24.57	35.48	23.86	0.00	1534.4
9	24.53	35.49	23.87	0.04	1534.4
15	24.49	35.49	23.90	0.07	1534.4
20	24.35	35.51	23.96	0.09	1534.2
35	23.26	35.71	24.42	0.14	1531.9
52	22.58	35.75	24.66	0.20	1530.4
74	21.08	35.68	25.02	0.27	1526.8
98	20.11	35.66	25.27	0.34	1524.5
129	19.10	35.63	25.51	0.42	1522.0
195	17.86	35.58	25.79	0.58	1519.5
258	16.42	35.47	26.04	0.72	1516.1
323	14.95	35.34	26.27	0.84	1512.2
386	13.43	35.18	26.47	0.95	1508.1
455	12.31	35.03	26.58	1.06	1505.2
511	11.21	34.90	26.69	1.15	1502.2
578	10.11	34.80	26.80	1.25	1499.2

This work is licensed under the Creative Commons Attribution-NonCommercial-NoDerivs 3.0 Unported License.
To view a copy of this license, visit http://creativecommons.org/licenses/by-nc-nd/3.0/

E502 (cont'd)

P	T	S	σ_t	$\Sigma\Delta D$	C
644	9.12	34.67	26.87	1.33	1496.6
718	8.48	34.62	26.93	1.43	1495.4
759	7.93	34.57	26.98	1.48	1493.8
933	6.51	34.47	27.09	1.68	1490.9
1249	4.39	34.48	27.37	1.99	1487.5
1523	3.30	34.57	27.54	2.19	1487.3

E503

P	T	S	σ_t	$\Sigma\Delta D$	C
0	23.77	35.63	24.22	0.00	1532.6
8	23.77	35.64	24.22	0.03	1532.7
17	23.71	35.64	24.24	0.06	1532.6
26	23.39	35.64	24.34	0.09	1532.0
34	22.56	35.64	24.58	0.12	1529.9
46	20.54	35.63	25.12	0.16	1524.7
78	19.26	35.61	25.45	0.25	1521.7
122	18.05	35.57	25.73	0.35	1518.8
136	16.93	35.52	25.96	0.38	1515.7
219	15.04	35.37	26.27	0.55	1511.0
319	13.11	35.20	26.55	0.72	1506.0
383	12.03	35.06	26.65	0.82	1503.1
459	10.85	34.92	26.77	0.93	1500.0
541	9.56	34.77	26.88	1.04	1496.6
602	8.86	34.70	26.94	1.11	1494.9
681	7.96	34.60	26.99	1.21	1492.7
775	7.17	34.54	27.05	1.32	1491.2
842	6.65	34.50	27.11	1.40	1491.1
914	6.22	34.48	27.14	1.48	1489.6
1141	4.71	34.49	27.33	1.70	1487.0
1550	3.29	34.58	27.55	2.02	1487.9
2011	2.43	34.64	27.68	2.30	1491.8

E504

P	T	S	σ_t	$\Sigma\Delta D$	C
0	23.59	35.66	24.29	0.00	1532.2
10	23.54	35.67	24.31	0.04	1532.3
21	23.52	35.67	24.32	0.08	1532.2
33	23.50	35.67	24.33	0.12	1532.4
56	22.92	35.67	24.50	0.20	1531.3
72	21.52	35.65	24.87	0.25	1527.9
94	20.12	35.62	25.23	0.32	1524.4
141	18.29	35.58	25.67	0.44	1519.9
188	17.38	35.54	25.86	0.55	1517.9
278	15.62	35.42	26.18	0.73	1513.7
379	13.77	35.25	26.45	0.91	1509.2
465	12.42	35.10	26.61	1.05	1506.0
546	10.99	34.93	26.76	1.17	1502.1
648	9.41	34.74	26.88	1.31	1497.6
737	8.34	34.62	26.95	1.42	1495.1
825	7.60	34.56	27.01	1.53	1493.6
925	6.76	34.51	27.09	1.65	1491.9
1035	6.10	34.47	27.15	1.77	1491.0
1106	5.62	34.47	27.21	1.85	1490.2
1379	4.03	34.52	27.43	2.09	1488.1
1876	2.70	34.61	27.63	2.43	1490.7
2352	2.26	34.66	27.71	2.69	1496.6

E505

P	T	S	σ_t	$\Sigma\Delta D$	C
0	22.98	35.61	24.43	0.00	1530.5
7	22.96	35.62	24.44	0.04	1530.6
17	22.78	35.62	24.49	0.07	1530.3
26	22.74	35.63	24.51	0.10	1530.3
43	20.75	35.63	25.06	0.15	1525.3
69	18.76	35.58	25.55	0.22	1520.0
104	17.79	35.54	25.76	0.31	1517.8
151	16.65	35.52	26.01	0.41	1515.0
185	15.83	35.44	26.14	0.48	1513.0
283	13.70	35.24	26.46	0.65	1507.4
380	12.11	35.05	26.62	0.81	1503.4
480	11.01	34.93	26.73	0.95	1501.0
558	9.58	34.76	26.86	1.06	1496.9
658	8.24	34.62	26.96	1.19	1493.4
758	7.39	34.55	27.03	1.31	1491.6
847	6.58	34.49	27.10	1.41	1490.0
949	6.00	34.48	27.16	1.52	1489.2
1062	5.34	34.47	27.24	1.63	1488.3
1135	4.94	34.47	27.28	1.70	1488.0

E505 (cont'd)

P	T	S	σ_t	$\Sigma\Delta D$	C
1423	3.81	34.52	27.44	1.94	1487.8
1937	2.54	34.62	27.64	2.29	1491.1
2424	2.20	34.66	27.71	2.55	1497.7

E506

P	T	S	σ_t	$\Sigma\Delta D$	C
0	22.38	35.61	24.59	0.00	1529.0
10	21.94	35.61	24.72	0.03	1528.0
20	21.55	35.61	24.83	0.06	1527.0
30	21.03	35.59	24.96	0.10	1525.9
49	19.49	35.58	25.37	0.15	1521.9
81	18.34	35.56	25.58	0.23	1519.1
109	16.83	35.52	25.97	0.29	1514.8
166	15.03	35.41	26.30	0.40	1510.1
193	14.28	35.35	26.41	0.45	1508.1
294	12.65	35.18	26.62	0.61	1504.1
394	11.13	34.99	26.76	0.76	1500.2
496	10.02	34.82	26.82	0.90	1497.7
570	8.95	34.68	26.89	0.99	1494.7
661	7.94	34.58	26.98	1.11	1492.2
756	7.12	34.53	27.05	1.22	1490.7
845	6.52	34.49	27.10	1.32	1489.6
948	5.93	34.47	27.16	1.43	1488.9
1037	5.25	34.47	27.25	1.51	1487.5
1126	4.72	34.48	27.31	1.60	1486.9
1432	3.46	34.54	27.49	1.84	1486.5
1909	2.54	34.62	27.64	2.15	1490.6
2376	2.24	34.65	27.69	2.40	1497.1

E507

P	T	S	σ_t	$\Sigma\Delta D$	C
0	21.36	35.47	24.78	0.00	1526.1
10	21.31	35.47	24.79	0.03	1526.2
20	20.43	35.46	25.03	0.06	1523.9
30	20.17	35.46	25.09	0.09	1523.3
50	19.81	35.46	25.18	0.14	1522.5
67	16.68	35.48	25.98	0.18	1513.8
99	15.59	35.48	26.22	0.25	1510.9
142	14.80	35.43	26.36	0.33	1509.0
183	14.48	35.40	26.41	0.40	1508.6
278	13.62	35.30	26.56	0.55	1507.1
372	12.37	35.13	26.64	0.70	1504.3
473	10.83	34.93	26.77	0.84	1500.3
551	9.61	34.76	26.85	0.95	1498.0
651	8.51	34.65	26.94	1.08	1494.3
744	7.63	34.57	27.01	1.19	1492.4
831	7.14	34.53	27.05	1.29	1491.9
936	6.30	34.49	27.13	1.41	1490.2
1056	5.63	34.48	27.21	1.53	1489.5
1122	5.15	34.47	27.26	1.60	1488.5
1413	3.90	34.51	27.43	1.85	1488.0
1909	2.75	34.62	27.63	2.19	1491.4
2380	2.23	34.66	27.70	2.45	1497.0

E508

P	T	S	σ_t	$\Sigma\Delta D$	C
0	21.43	35.38	24.69	0.00	1526.2
10	20.81	35.39	24.87	0.03	1524.7
20	20.18	35.40	25.04	0.06	1523.2
30	19.99	35.40	25.09	0.09	1522.8
48	18.53	35.40	25.46	0.14	1518.9
73	17.57	35.38	25.69	0.20	1516.5
98	15.45	35.37	26.18	0.25	1510.3
140	14.01	35.32	26.45	0.33	1506.3
187	13.48	35.27	26.52	0.40	1505.2
271	12.42	35.14	26.63	0.53	1502.9
355	11.18	34.98	26.75	0.65	1499.8
463	9.86	34.81	26.85	0.80	1496.4
545	8.89	34.69	26.91	0.90	1494.2
612	8.21	34.63	26.97	0.99	1492.4
799	6.89	34.53	27.13	1.20	1490.3
894	6.29	34.51	27.19	1.30	1489.6
996	5.67	34.50	27.22	1.40	1488.7
1052	5.34	34.49	27.25	1.45	1488.2
1294	4.08	34.51	27.40	1.66	1487.0
1739	2.84	34.60	27.60	1.98	1489.1

This work is licensed under the Creative Commons Attribution-NonCommercial-NoDerivs 3.0 Unported License.
To view a copy of this license, visit http://creativecommons.org/licenses/by-nc-nd/3.0/

E509

P	T	S	σ_t	$\Sigma\Delta D$	C
0	21.23	35.32	24.69	0.00	1525.9
9	20.60	35.39	24.92	0.03	1524.1
18	20.13	35.41	25.06	0.06	1523.0
27	19.56	35.42	25.22	0.08	1521.4
45	18.36	35.42	25.52	0.13	1518.3
65	16.65	35.42	25.94	0.17	1513.5
87	15.29	35.42	26.25	0.22	1509.7
139	14.09	35.34	26.45	0.31	1506.5
166	13.75	35.28	26.48	0.35	1505.8
270	12.25	35.11	26.64	0.51	1502.2
386	11.24	34.98	26.73	0.68	1500.5
430	10.37	34.86	26.80	0.74	1497.9
494	9.03	34.71	26.90	0.82	1493.9
588	8.06	34.63	26.99	0.94	1491.5
663	7.50	34.58	27.04	1.02	1490.5
750	6.81	34.53	27.10	1.12	1489.3
831	6.28	34.49	27.13	1.21	1488.5
1091	4.72	34.48	27.31	1.46	1486.3
1510	3.44	34.56	27.51	1.79	1487.9
1955	2.58	34.61	27.63	2.06	1491.6

E510

P	T	S	σ_t	$\Sigma\Delta D$	C
0	23.94	35.67	24.19	0.00	1533.1
8	23.83	35.68	24.22	0.03	1532.9
16	23.50	35.68	24.32	0.06	1532.2
24	23.39	35.68	24.36	0.09	1532.1
38	22.84	35.67	24.52	0.14	1530.9
64	19.92	35.62	25.28	0.23	1523.3
113	18.40	35.58	25.63	0.36	1519.7
151	16.73	35.50	25.98	0.44	1515.2
183	15.90	35.45	26.14	0.51	1512.9
285	13.76	35.26	26.46	0.69	1507.7
387	12.20	35.10	26.64	0.85	1505.9
479	10.66	34.91	26.78	0.98	1499.7
600	8.96	34.70	26.91	1.14	1495.3
666	8.26	34.64	26.97	1.23	1493.5
763	7.32	34.56	27.04	1.34	1491.5
848	6.75	34.54	27.12	1.44	1490.6
953	6.14	34.51	27.17	1.55	1489.8
1055	5.35	34.50	27.26	1.65	1488.4
1135	4.93	34.51	27.31	1.72	1487.9
1418	3.53	34.55	27.49	1.94	1486.6
1939	2.54	34.62	27.64	2.29	1491.1
2414	2.20	34.65	27.70	2.54	1497.5

E511

P	T	S	σ_t	$\Sigma\Delta D$	C
0	23.72	35.63	24.23	0.00	1532.5
5	23.55	35.64	24.27	0.02	1532.1
10	23.33	35.69	24.39	0.04	1531.7
15	22.88	35.69	24.51	0.05	1530.6
28	22.02	35.70	24.76	0.10	1528.6
41	20.33	35.71	25.24	0.14	1524.3
70	19.72	35.70	25.39	0.21	1522.9
187	17.55	35.65	25.90	0.51	1518.4
241	17.16	35.61	25.97	0.62	1518.1
310	16.64	35.56	26.04	0.77	1517.6
374	15.85	35.47	26.16	0.90	1516.2
438	14.40	35.32	26.37	1.02	1512.3
624	10.19	34.86	26.83	1.31	1500.5
723	8.81	34.71	26.94	1.44	1496.0
869	7.31	34.58	27.06	1.62	1493.0
936	6.81	34.54	27.11	1.69	1492.2
1376	4.37	34.50	27.37	2.12	1489.5
1669	3.23	34.57	27.54	2.34	1489.5

E512

P	T	S	σ_t	$\Sigma\Delta D$	C
0	24.34	35.60	24.02	0.00	1534.0
8	23.71	35.61	24.21	0.03	1532.4
16	23.40	35.62	24.31	0.06	1531.9
24	22.43	35.61	24.58	0.09	1529.5
39	20.64	35.59	25.06	0.14	1524.9
61	18.15	35.57	25.69	0.19	1518.2
103	17.35	35.57	25.89	0.29	1516.4
135	16.39	35.49	26.11	0.35	1514.0
167	15.53	35.41	26.18	0.41	1511.7

E512 (cont'd)

P	T	S	σ_t	$\Sigma\Delta D$	C
262	14.06	35.28	26.44	0.58	1508.3
356	12.37	35.09	26.66	0.73	1504.0
445	10.58	34.86	26.77	0.86	1498.9
515	9.57	34.75	26.85	0.95	1496.3
609	8.54	34.65	26.93	1.07	1493.8
699	7.45	34.56	27.03	1.18	1490.9
776	6.97	34.52	27.07	1.27	1490.3
874	6.44	34.48	27.10	1.38	1489.8
982	5.63	34.47	27.20	1.49	1488.2
1069	5.11	34.47	27.26	1.58	1487.3
1308	3.91	34.49	27.41	1.78	1486.4
1771	2.81	34.58	27.58	2.11	1489.3
2222	2.31	34.62	27.67	2.38	1494.7

E513

P	T	S	σ_t	$\Sigma\Delta D$	C
0	25.07	35.55	23.76	0.00	1535.7
7	25.05	35.56	23.89	0.03	1535.8
13	25.00	35.56	23.90	0.05	1535.7
19	24.11	35.68	24.14	0.08	1533.7
33	23.14	35.70	24.44	0.13	1531.5
40	21.62	35.69	24.87	0.15	1527.6
65	18.83	35.63	25.57	0.22	1520.2
97	18.02	35.62	25.75	0.30	1518.5
129	17.46	35.59	25.88	0.37	1517.1
201	16.39	35.49	26.06	0.52	1515.0
273	14.96	35.37	26.28	0.66	1511.4
333	14.02	35.27	26.40	0.76	1509.3
393	13.07	35.14	26.50	0.86	1507.0
455	11.89	35.01	26.64	0.96	1503.8
555	10.30	34.84	26.79	1.11	1499.6
620	9.22	34.70	26.87	1.20	1496.6
684	8.20	34.61	26.95	1.28	1493.7
738	7.37	34.54	27.03	1.34	1491.2
804	6.78	34.51	27.08	1.42	1490.1
1041	4.82	34.46	27.29	1.66	1485.8
1391	3.37	34.54	27.51	1.93	1485.5
1683	2.77	34.60	27.61	2.12	1487.8

E514

P	T	S	σ_t	$\Sigma\Delta D$	C
0	25.86	35.55	23.52	0.00	1537.6
6	25.83	35.56	23.53	0.03	1537.6
12	25.79	35.56	23.54	0.05	1537.7
19	25.54	35.58	23.64	0.08	1537.2
34	25.00	35.60	23.82	0.15	1536.0
48	24.51	35.62	23.98	0.20	1535.1
60	22.21	35.63	24.71	0.25	1529.5
89	21.69	35.65	24.82	0.34	1528.5
118	20.49	35.66	25.15	0.43	1525.9
188	18.45	35.62	25.64	0.61	1521.1
258	17.23	35.51	25.87	0.78	1518.4
314	16.46	35.43	26.00	0.90	1517.0
375	15.24	35.38	26.28	1.02	1514.2
448	13.90	35.23	26.41	1.16	1510.7
496	12.10	35.06	26.63	1.24	1505.3
557	10.54	34.84	26.75	1.33	1500.5
620	9.53	34.72	26.84	1.41	1497.7
706	8.38	34.60	26.93	1.53	1494.7
751	7.62	34.52	26.97	1.58	1492.4
918	6.04	34.45	27.13	1.77	1488.8
1112	4.98	34.47	27.28	1.96	1487.7
1317	3.81	34.51	27.44	2.14	1486.1

E515

P	T	S	σ_t	$\Sigma\Delta D$	C
0	25.73	35.60	23.59	0.00	1537.3
10	25.68	35.61	23.62	0.04	1537.4
20	25.59	35.62	23.65	0.09	1537.3
30	24.85	35.66	23.91	0.13	1535.8
50	23.15	35.73	24.47	0.20	1531.8
67	21.40	35.70	24.94	0.26	1527.5
105	19.84	35.65	25.33	0.37	1523.8
157	18.37	35.62	25.67	0.50	1520.4
197	17.79	35.59	25.80	0.59	1519.4
295	16.47	35.48	26.02	0.81	1516.8
389	14.64	35.29	26.29	0.99	1512.3
504	12.40	35.04	26.57	1.19	1506.5

This work is licensed under the Creative Commons Attribution-NonCommercial-NoDerivs 3.0 Unported License.
To view a copy of this license, visit http://creativecommons.org/licenses/by-nc-nd/3.0/

E515 (cont'd)

P	T	S	σ_t	$\Sigma\Delta D$	C
582	10.81	34.87	26.73	1.31	1501.8
689	9.04	34.71	26.90	1.46	1497.0
783	7.92	34.59	26.98	1.58	1494.2
878	6.82	34.50	27.07	1.69	1491.3
983	6.08	34.46	27.14	1.80	1490.0
1107	5.20	34.45	27.23	1.93	1487.4
1171	4.66	34.46	27.31	1.99	1487.2
1464	3.49	34.54	27.49	2.23	1487.3
1987	2.49	34.62	27.65	2.56	1491.6
2477	2.12	34.66	27.71	2.83	1498.2

E516

P	T	S	σ_t	$\Sigma\Delta D$	C
0	25.33	35.57	23.70	0.00	1536.3
5	25.33	35.58	23.70	0.02	1536.4
10	25.29	35.58	23.71	0.04	1536.5
16	25.28	35.58	23.72	0.07	1536.6
28	24.66	35.63	23.94	0.12	1535.2
48	22.39	35.67	24.64	0.19	1529.9
74	21.43	35.65	24.89	0.27	1527.7
117	20.01	35.63	25.25	0.40	1524.4
149	18.96	35.62	25.53	0.48	1521.9
191	17.67	35.60	25.83	0.58	1518.9
254	16.65	35.50	26.00	0.72	1516.7
306	15.95	35.43	26.16	0.83	1515.2
382	14.49	35.32	26.35	0.97	1511.7
448	13.23	35.18	26.50	1.08	1508.2
513	11.95	35.03	26.69	1.19	1504.9
572	10.76	34.89	26.75	1.28	1501.6
643	9.80	34.78	26.83	1.38	1499.1
722	9.06	34.72	26.91	1.48	1497.5
780	8.53	34.66	26.95	1.56	1496.5
958	6.77	34.53	27.10	1.77	1492.4
1304	4.36	34.50	27.27	2.12	1488.3
1651	3.08	34.58	27.56	2.40	1488.6

E517

P	T	S	σ_t	$\Sigma\Delta D$	C
0	24.73	35.63	23.92	0.00	1534.9
10	23.83	35.60	24.16	0.04	1532.9
21	23.17	35.60	24.36	0.08	1531.3
32	21.91	35.60	24.72	0.12	1528.2
56	19.03	35.57	25.47	0.19	1520.6
76	17.73	35.55	25.78	0.23	1517.1
111	17.27	35.54	25.88	0.31	1516.3
164	15.98	35.46	26.12	0.42	1513.2
205	14.72	35.35	26.32	0.50	1509.6
305	13.24	35.19	26.51	0.67	1506.3
405	11.91	35.04	26.66	0.82	1503.1
506	10.34	34.85	26.80	0.97	1499.0
620	9.17	34.72	26.89	1.12	1496.4
696	8.52	34.66	26.95	1.21	1495.1
790	7.68	34.58	27.01	1.33	1493.3
890	6.60	34.51	27.10	1.44	1490.7
989	5.78	34.45	27.17	1.55	1488.9
1090	5.13	34.44	27.23	1.65	1487.9
1174	4.68	34.46	27.31	1.73	1487.5
1473	3.43	34.55	27.50	1.97	1487.1
1949	2.46	34.61	27.64	2.27	1490.8
2392	2.12	34.65	27.70	2.51	1496.8

E518

P	T	S	σ_t	$\Sigma\Delta D$	C
0	23.96	35.66	24.18	0.00	1533.1
10	23.05	35.66	24.44	0.04	1531.0
20	22.73	35.66	24.54	0.07	1530.2
30	21.28	35.64	24.93	0.10	1526.6
57	20.15	35.64	25.23	0.18	1523.7
71	19.30	35.60	25.42	0.22	1521.6
131	18.04	35.57	25.72	0.37	1518.9
171	17.21	35.54	25.89	0.46	1517.0
201	16.71	35.51	26.00	0.52	1515.9
302	14.78	35.35	26.31	0.72	1511.4
403	13.37	35.23	26.51	0.89	1508.3
506	11.86	35.06	26.69	1.05	1504.7
589	10.01	34.81	26.82	1.17	1499.0
701	9.04	34.71	26.90	1.32	1497.2
796	7.99	34.60	26.98	1.44	1494.6

E518 (cont'd)

P	T	S	σ_t	$\Sigma\Delta D$	C
900	6.88	34.52	27.08	1.56	1492.0
1002	6.37	34.49	27.12	1.67	1491.6
1112	5.67	34.48	27.20	1.79	1490.6
1185	5.17	34.48	27.26	1.86	1489.6
1489	3.85	34.52	27.44	2.13	1489.1
2002	2.59	34.61	27.63	2.49	1492.3
2500	2.22	34.64	27.68	2.77	1499.0

E519

P	T	S	σ_t	$\Sigma\Delta D$	C
0	23.15	35.49	24.29	0.00	1530.8
5	22.94	35.51	24.37	0.02	1530.4
10	22.40	35.51	24.52	0.04	1529.1
15	21.81	35.51	24.68	0.05	1527.3
22	21.07	35.51	24.89	0.07	1525.8
39	20.71	35.50	24.97	0.13	1524.9
55	19.90	35.49	25.18	0.17	1523.0
152	16.36	35.40	26.00	0.41	1514.0
179	15.30	35.37	26.26	0.46	1511.1
276	14.00	35.31	26.44	0.63	1508.4
372	12.75	35.10	26.54	0.79	1505.6
446	11.75	35.03	26.67	0.90	1503.5
550	10.66	34.90	26.77	1.05	1500.9
605	9.91	34.83	26.86	1.13	1499.0
685	9.00	34.73	26.93	1.23	1496.9
790	7.87	34.60	27.00	1.36	1494.1
898	6.51	34.53	27.13	1.49	1490.4
1144	4.95	34.51	27.31	1.73	1488.1
1648	3.07	34.59	27.57	2.12	1488.5
2038	2.51	34.62	27.64	2.35	1492.4

E520

P	T	S	σ_t	$\Sigma\Delta D$	C
0	20.72	35.40	24.89	0.00	1524.3
10	18.85	35.38	25.36	0.03	1519.2
22	18.11	35.37	25.54	0.06	1517.2
34	17.32	35.35	25.73	0.10	1515.0
56	16.72	35.35	25.87	0.15	1513.6
72	16.28	35.35	25.98	0.20	1512.5
109	15.63	35.35	26.12	0.31	1511.0
160	14.89	35.34	26.28	0.41	1509.6
203	13.71	35.25	26.46	0.48	1506.1
308	12.47	35.11	26.60	0.65	1503.5
413	11.32	34.98	26.72	0.80	1501.1
509	9.93	34.80	26.83	0.94	1497.5
600	8.96	34.70	26.91	1.06	1495.3
705	8.05	34.62	26.98	1.19	1493.4
810	7.22	34.55	27.06	1.32	1491.9
911	6.56	34.52	27.12	1.43	1490.8
1011	5.89	34.49	27.19	1.54	1489.8
1131	5.25	34.49	27.26	1.66	1489.1
1210	4.80	34.50	27.37	1.73	1488.6
1493	3.57	34.55	27.49	1.95	1488.1
1786	2.67	34.60	27.61	2.17	1489.1

E521

P	T	S	σ_t	$\Sigma\Delta D$	C
0	23.46	35.72	24.43	0.00	1531.8
9	23.10	35.72	24.53	0.03	1531.0
18	22.75	35.71	24.57	0.07	1530.3
27	22.17	35.70	24.72	0.10	1529.0
48	20.15	35.65	25.24	0.16	1523.8
74	18.27	35.61	25.70	0.23	1518.8
98	16.77	35.57	26.03	0.28	1514.7
156	16.13	35.54	26.15	0.40	1513.6
192	15.55	35.51	26.26	0.46	1512.3
293	15.05	35.47	26.34	0.65	1512.3
393	13.52	35.25	26.55	0.82	1508.7
491	12.20	35.07	26.62	0.97	1507.6
582	10.84	34.91	26.75	1.11	1502.0
681	9.30	34.73	26.88	1.25	1498.0
775	8.25	34.63	26.97	1.37	1495.3
866	7.52	34.56	27.02	1.48	1494.0
965	6.91	34.52	27.08	1.60	1493.5
1079	6.16	34.49	27.15	1.72	1491.9
1169	5.59	34.47	27.20	1.82	1491.1
1425	4.04	34.52	27.42	2.05	1489.0
1925	2.66	34.62	27.63	2.40	1491.3
2372	2.18	34.65	27.70	2.64	1496.7

This work is licensed under the Creative Commons Attribution-NonCommercial-NoDerivs 3.0 Unported License.
To view a copy of this license, visit http://creativecommons.org/licenses/by-nc-nd/3.0/

HYDROLOGY OF THE NORTH-EAST TASMAN SEA

by

D. M. Garner

New Zealand Oceanographic Institute

ABSTRACT

The distribution of ocean temperature and salinity in the north-east Tasman Sea, west of North Island, New Zealand, is described. Based on these data, calculations are made of the geostrophic circulation and of the velocity of sound in this region. This study was the fifth of a series of block surveys of oceanic hydrology in the New Zealand region.

INTRODUCTION

During March 1967 the fifth contribution to a series of studies on the summer distribution of temperature and salinity in ocean waters around New Zealand covered a block in the north-east Tasman Sea to the west of North Island, between latitudes 35° 30′ S and 39° 30′ S, and between longitudes 164° 30′ E and 172° 30′ E. Earlier work in this series has been reported by Garner (1967a, b) and by Ridgway (in press) and Garner (in this volume). The grid of 21 stations worked extended from the south-eastern end of the New Caledonia Basin, across the Lord Howe Rise, to the north-eastern margin of the Tasman Basin. The configurations of bottom topography and station positions are shown in Fig. 1. The bathythermograph and reversing bottles with thermometers were used to define temperature and salinity of ocean waters as a function of pressure over the survey area. Methods of working followed those described in earlier reports of this series of studies.

PRESENTATION OF DATA

Positions and times of stations are listed in Table 1 together with meteorological information. Observed station depth/temperature/salinity data are listed in the Appendix together with derived values of density, geopotential anomaly, and sound velocity computed according to relations given by LaFond (1951) and Wilson (1960). Tracings of bathythermograph records are set out in Fig. 6.

This work is licensed under the Creative Commons Attribution-NonCommercial-NoDerivs 3.0 Unported License.
To view a copy of this license, visit http://creativecommons.org/licenses/by-nc-nd/3.0/

TABLE 1. Station Circumstances

Air (screen) temperature and wind were estimated at bridge level.

Station No.	N.Z. Date/Time March 1967		Air Temp. (°C)	Wind		Latitude S	Longitude E
	Start	Finish		Dirn. (°T)	Speed (kt)		
F 799	3/0118	3/0438	15.7	110	5	38° 30′	165° 00′
F 800	3/1242	3/1450	17.2	080	7	39° 30′	164° 30′
F 801	3/2258	4/0112	16.0	080	10	39° 30′	165° 50′
F 802	4/0800	4/0920	17.5	040	11	39° 30′	167° 00′
F 803	4/1745	4/1904	18.7	020	17	39° 20′	168° 15′
F 804	5/0444	5/0544	19.2	020	13	38° 20′	168° 50′
F 805	5/1205	5/1355	20.1	045	7	38° 24′	167° 31′
F 806	5/2104	5/2253	18.0	200	8	38° 30′	166° 10′
F 807	6/0618	6/0747	18.9	140	15	37° 30′	165° 40′
F 808	6/1736	6/1937	19.9	080	15	36° 30′	166° 30′
F 809	7/1532	7/1723	21.5	050	13	35° 30′	167° 30′
F 810	8/0638	8/0817	20.5	040	15	35° 30′	169° 00′
F 811	8/1550	8/1746	20.3	040	10	36° 30′	168° 30′
F 812	9/0211	9/0330	20.1	050	9	37° 30′	167° 50′
F 813	9/1424	9/1605	20.4	020	10	37° 21′	169° 30′
F 814	9/2352	10/0132	20.0	030	10	35° 30′	170° 10′
F 815	10/1030	10/1236	20.6	020	16	35° 30′	170° 40′
F 816	10/2143	11/0057	21.2	030	10	36° 00′	172° 10′
F 817	11/0715	11/0904	20.7	350	15	36° 45′	171° 20′
F 818	11/1616	11/1754	20.0	280	15	37° 20′	172° 30′
F 819	12/0818	12/1040	17.0	170	25	38° 00′	171° 30′

This work is licensed under the Creative Commons Attribution-NonCommercial-NoDerivs 3.0 Unported License.
To view a copy of this license, visit http://creativecommons.org/licenses/by-nc-nd/3.0/

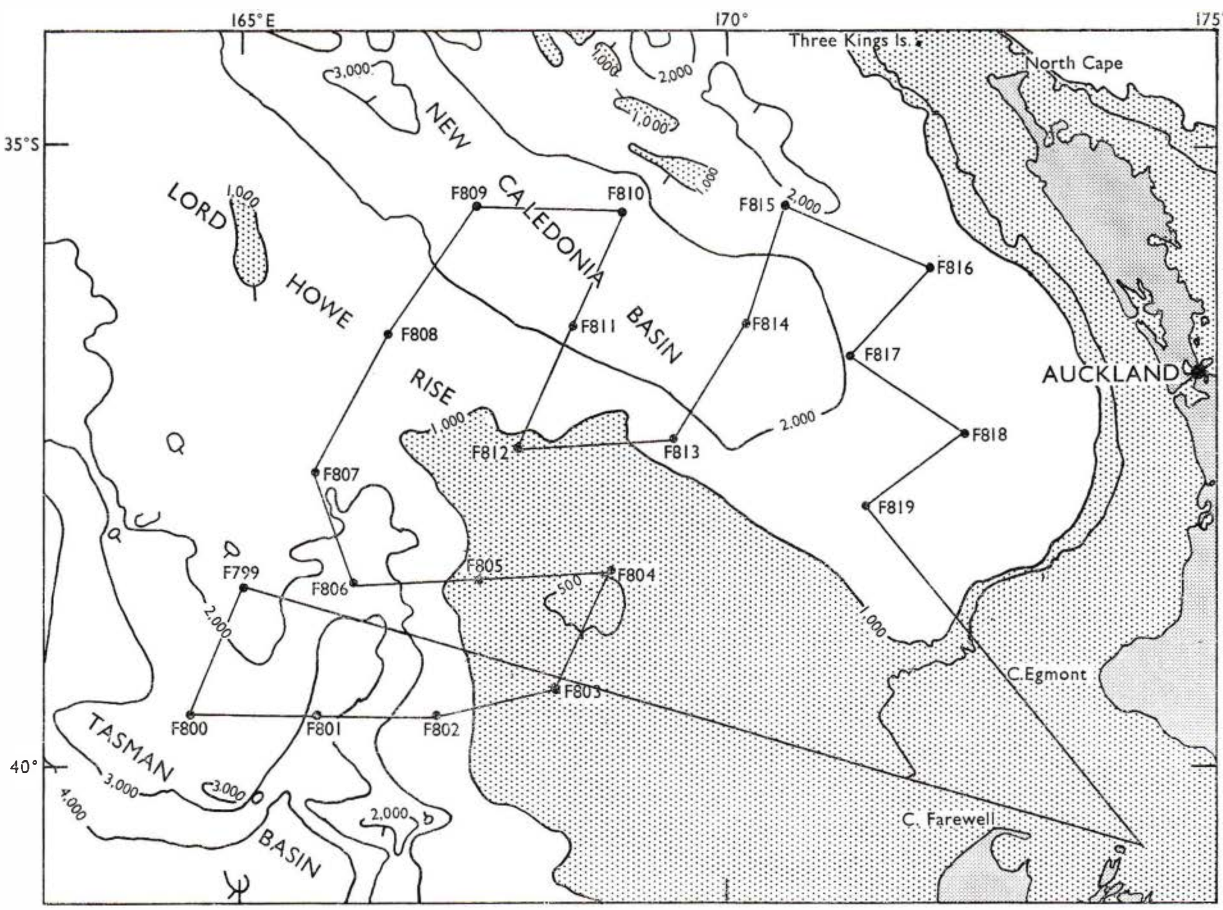

FIG. 1. The survey area showing station positions, ship's track, and isobaths (m) of the sea floor.

This work is licensed under the Creative Commons Attribution-NonCommercial-NoDerivs 3.0 Unported License.
To view a copy of this license, visit http://creativecommons.org/licenses/by-nc-nd/3.0/

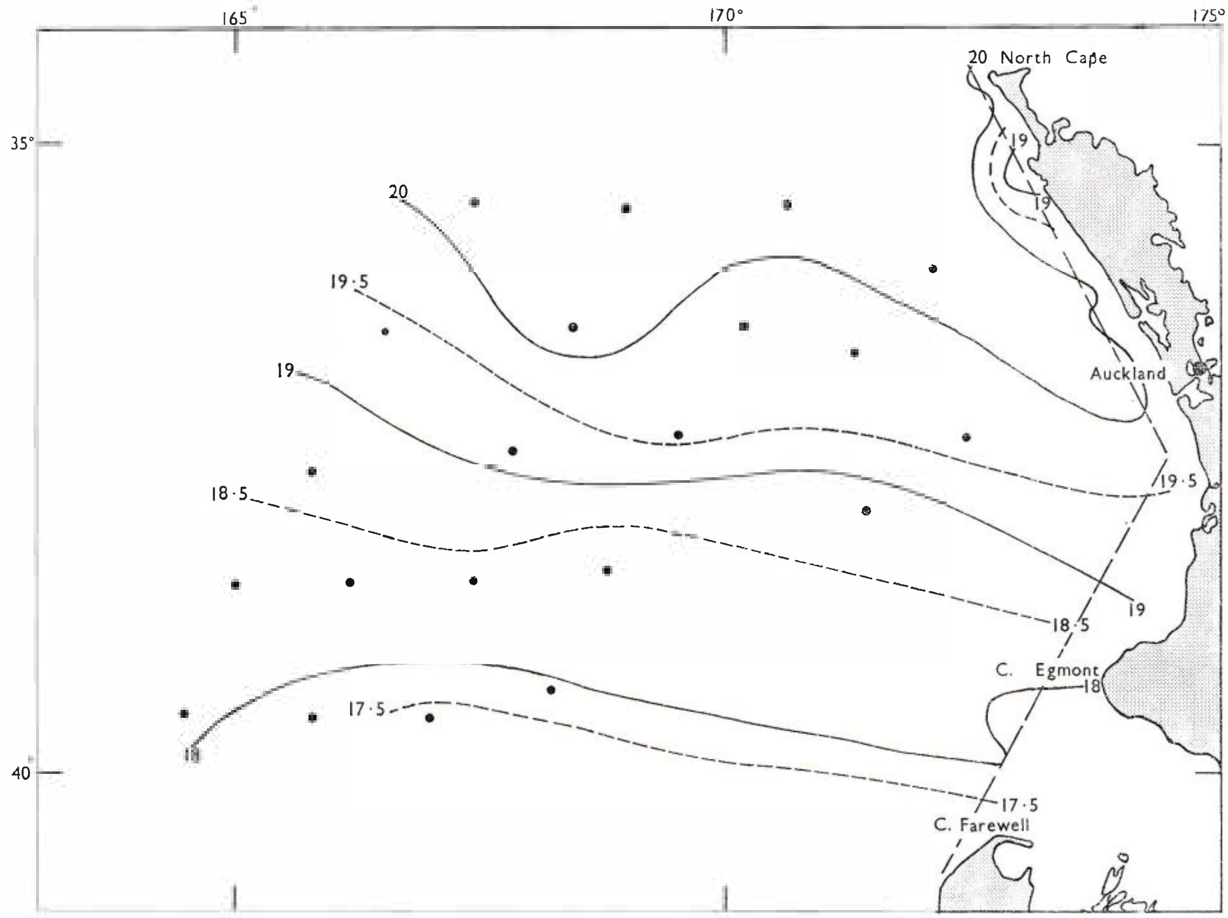

FIG. 2. Sea surface isotherms (°C).

This work is licensed under the Creative Commons Attribution-NonCommercial-NoDerivs 3.0 Unported License.
To view a copy of this license, visit http://creativecommons.org/licenses/by-nc-nd/3.0/

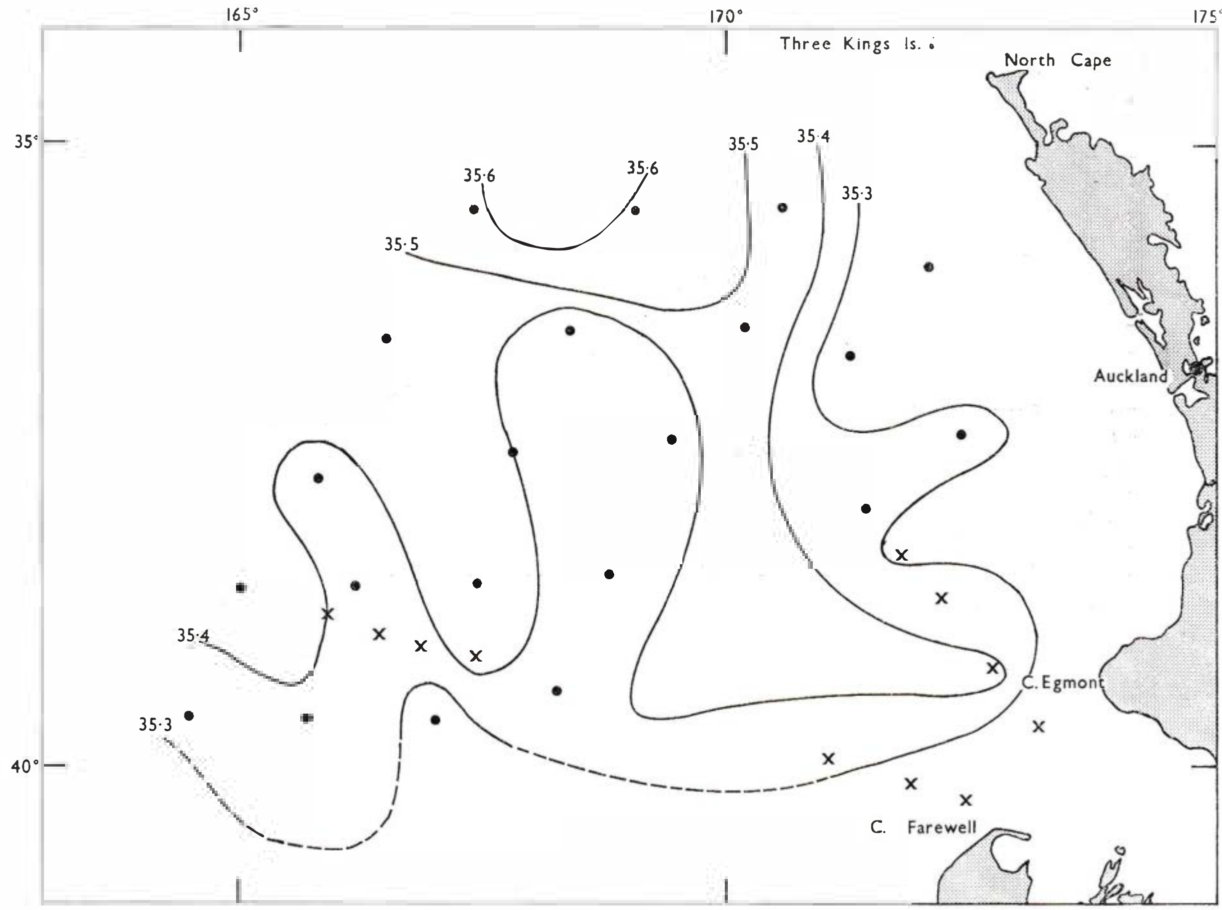

FIG. 3. Sea surface isohalines (‰). Crosses mark positions of water samples taken in addition to those at the stations marked by dots.

This work is licensed under the Creative Commons Attribution-NonCommercial-NoDerivs 3.0 Unported License.
To view a copy of this license, visit http://creativecommons.org/licenses/by-nc-nd/3.0/

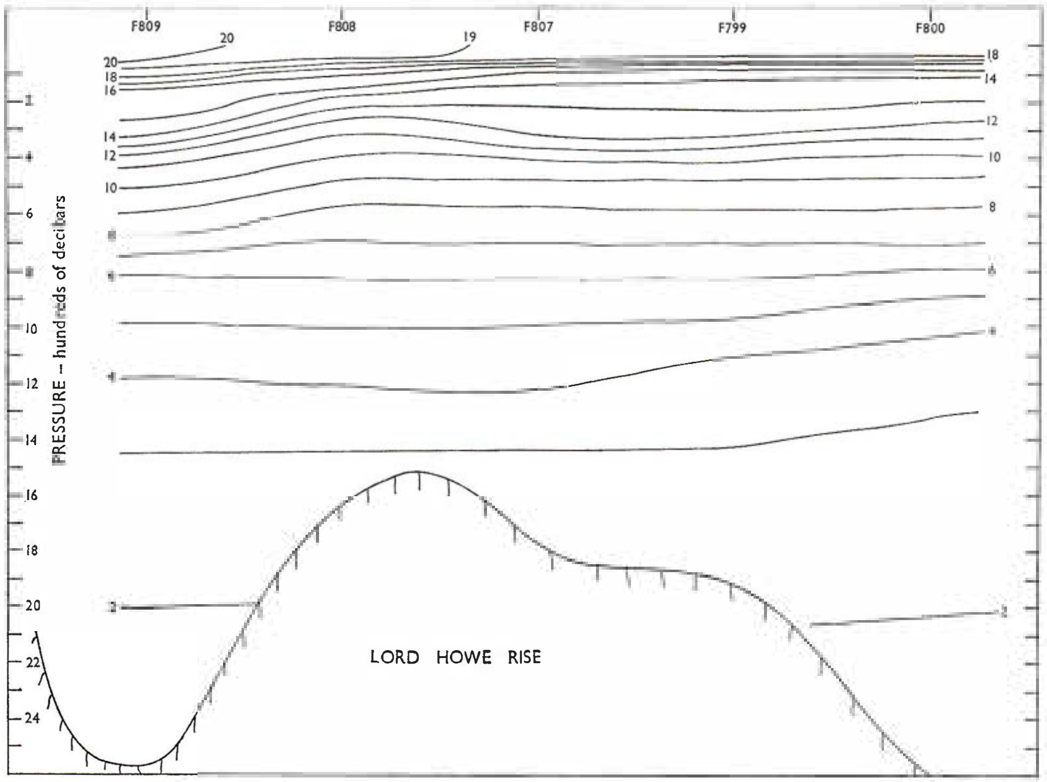

FIG. 4. Vertical cross section of temperature (°C) across Lord Howe Rise in the west of the survey area.

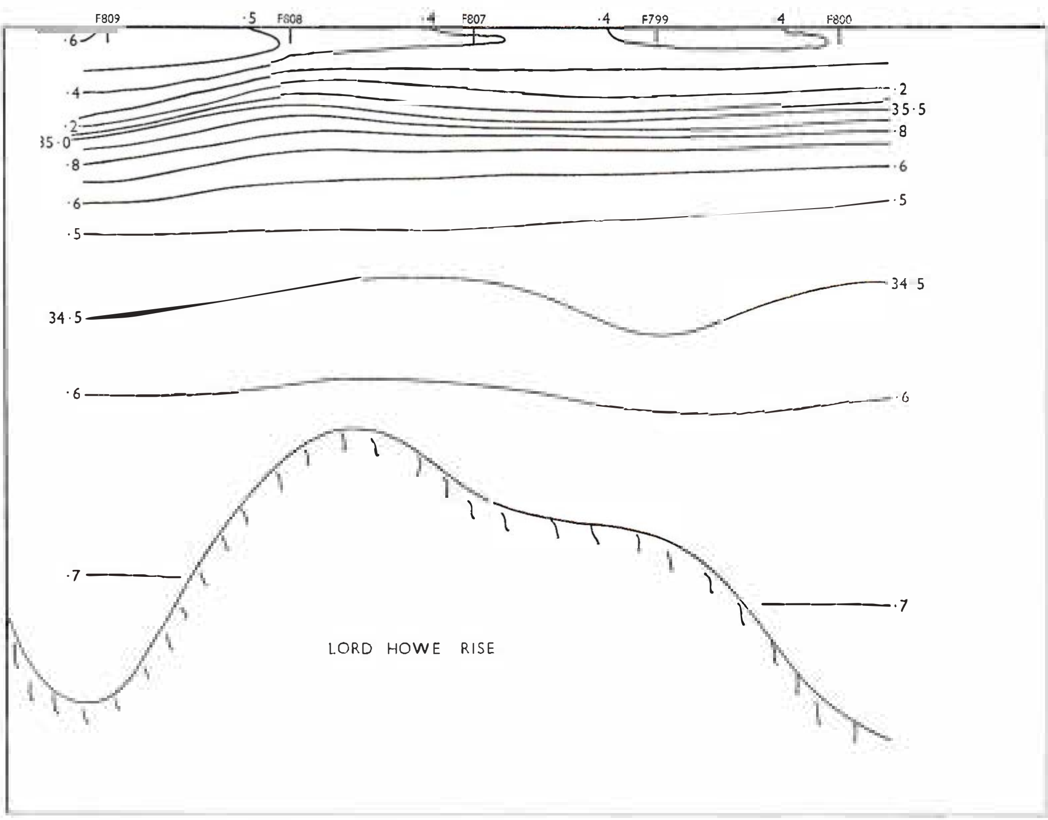

FIG. 5. Vertical cross section of salinity (‰) corresponding to the temperature section of Fig. 4.

This work is licensed under the Creative Commons Attribution-NonCommercial-NoDerivs 3.0 Unported License.
To view a copy of this license, visit http://creativecommons.org/licenses/by-nc-nd/3.0/

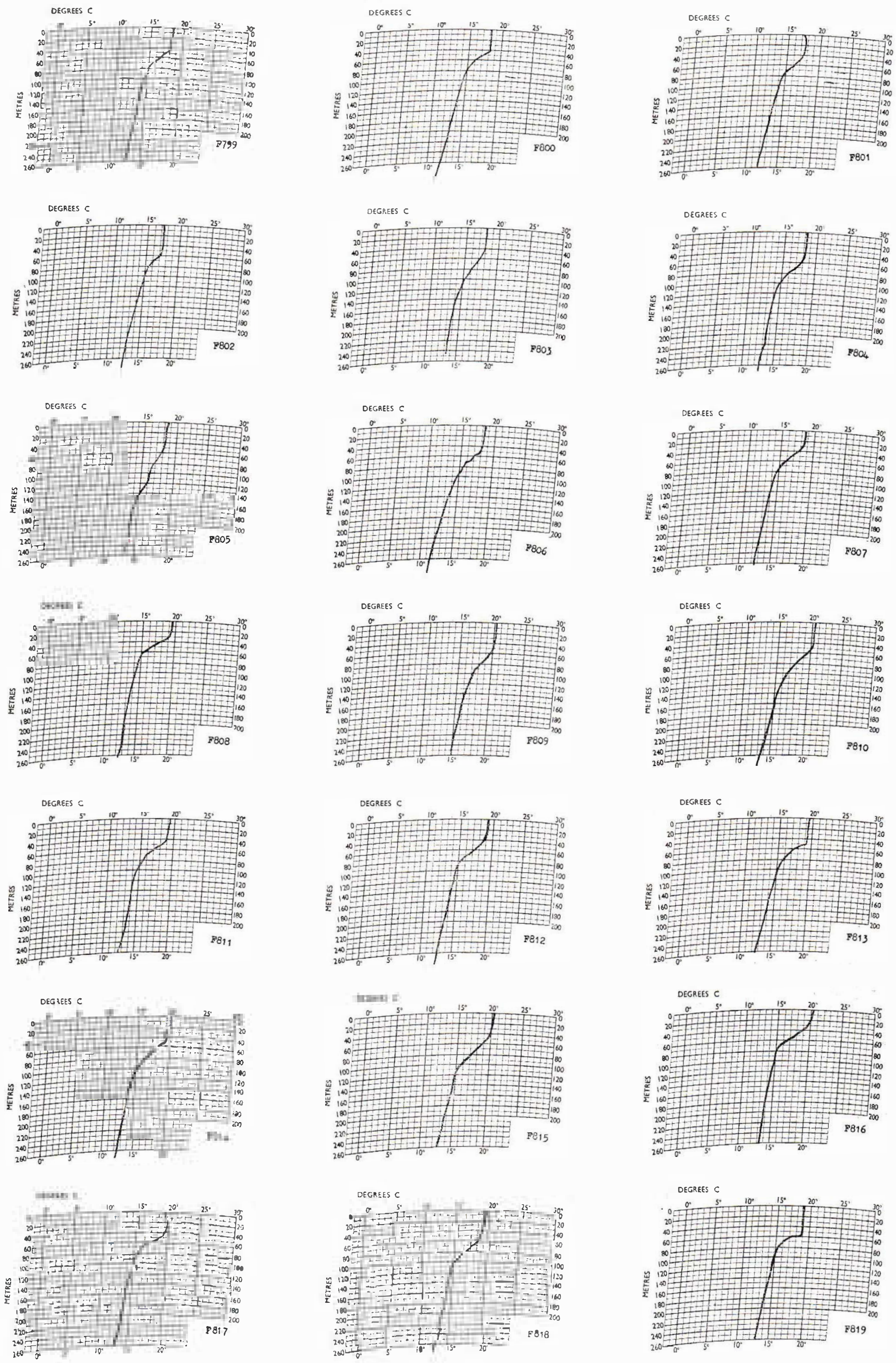

FIG. 6. Bathythermograph traces.

This work is licensed under the Creative Commons Attribution-NonCommercial-NoDerivs 3.0 Unported License.
To view a copy of this license, visit http://creativecommons.org/licenses/by-nc-nd/3.0/

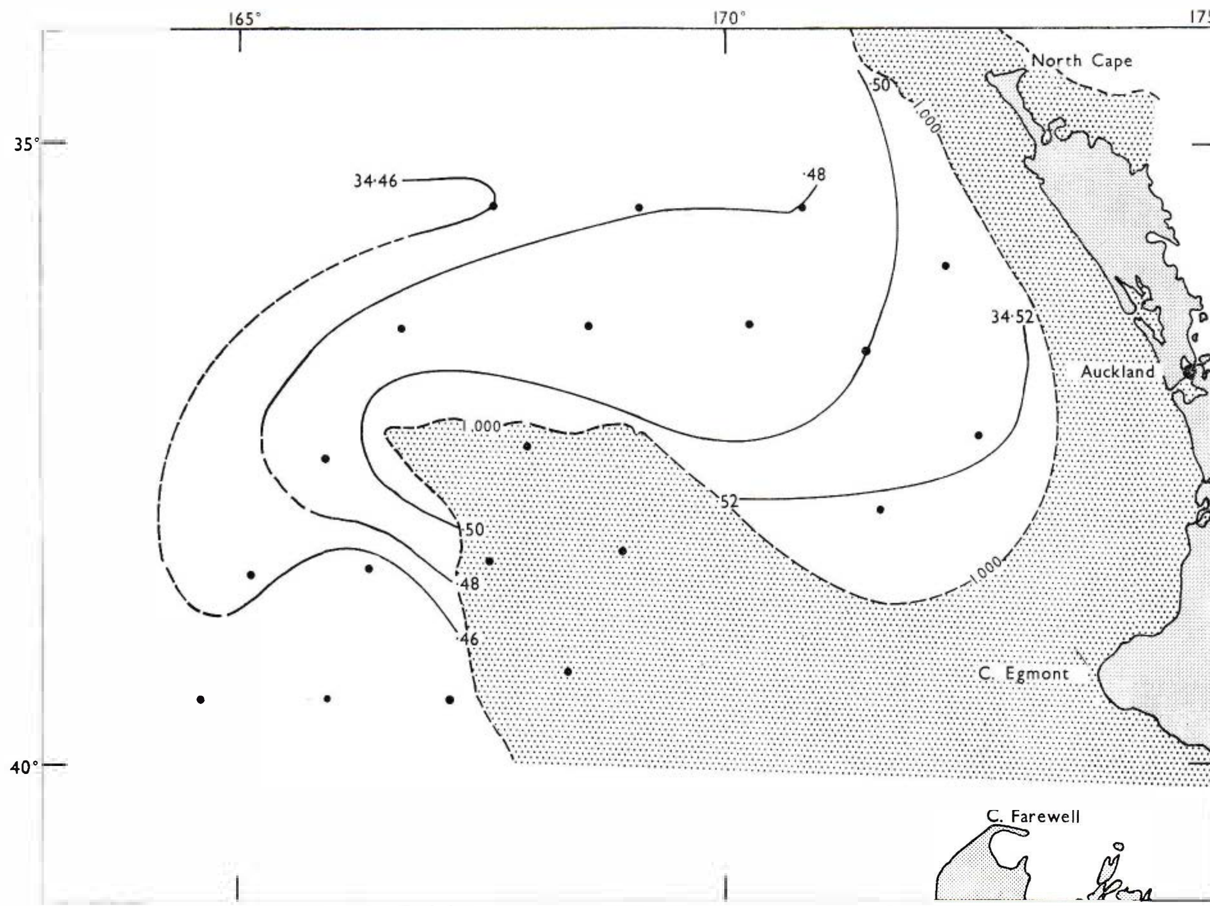

FIG. 7. Salinity at the core of the Antarctic Intermediate Water.

DISCUSSION

From the results of hydrological surveys north-west of New Zealand and in the south-east Tasman Sea (Garner, this volume; 1967b) it was apparent that rather small horizontal variations of water properties would be found over the present survey area in the north-east Tasman Sea. Very little structure is, in fact, revealed in the hydrological distributions mapped by this work, but the completion of this block provides a systematic description of the summer oceanic hydrology of a region extending some 300 miles westwards from New Zealand between latitudes 27° S and 48° S, within the limitations imposed by the use of data taken in different years. Present knowledge of the geopotential topography of the ocean surface in this area with respect to the 1,000 decibar isobaric surface has been summarised elsewhere (Garner, 1969b) from the data from this series of surveys. The present discussion is confined to a description of the hydrological characteristics of the north-east Tasman block.

SURFACE TEMPERATURE AND SALINITY

Figs. 2 and 3 provide, respectively, a description of the temperature and salinity of the sea surface over the survey area. Surface isotherms ran nearly east-west with a small and nearly constant meridional temperature gradient. The trend of isotherms between the survey area and the west coast of North Island has been estimated in Fig. 2 using a thermograph record obtained along the coast from m.v. *Taranui* just before working the survey block (Garner, 1969). No simple correlation between surface temperature and salinity was apparent. Isohalines were approximately zonally oriented in the west of the survey block but had a more north-south trend in the

This work is licensed under the Creative Commons Attribution-NonCommercial-NoDerivs 3.0 Unported License.
To view a copy of this license, visit http://creativecommons.org/licenses/by-nc-nd/3.0/

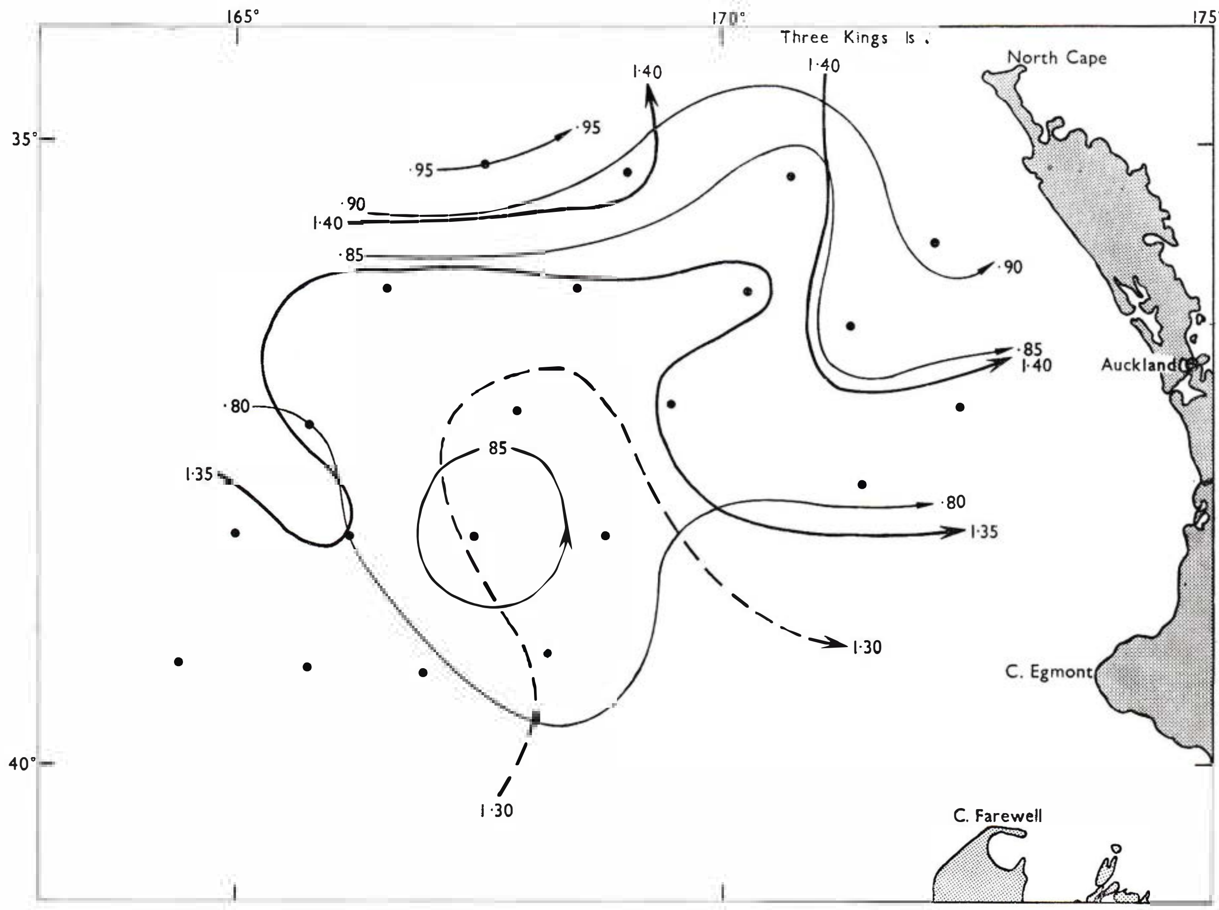

FIG. 8. Geopotential topography of the sea surface estimated with respect to (a) 1,000 decibars (heavy black) and (b) 500 decibars (light black) in dynamic metres. Contours are also streamlines of the relative surface geostrophic circulation in the sense of the arrows.

east. Measurements along *Taranui's* coastal passage showed that surface salinity continued to fall between the survey block and the shelf but contained so much detail due to coastal fresh water run-off that the isohalines in Fig. 3 could not readily be continued eastwards.

SUBSURFACE TEMPERATURE AND SALINITY

Figs. 4 and 5 show isotherms and isohalines, respectively, in vertical cross section along the westernmost line of stations in the survey area. An isothermal upper mixed layer about 50 m deep covered the area. The bathythermograph traces of Fig. 6 show that the lower boundary of this layer was well defined. A discontinuity in vertical temperature gradient occurred at the top of the thermocline layer at all stations except for the group F 803, F 804, and F 805 over the eastern end of the Lord Howe Rise. Salinity in the upper mixed layer tended to increase slightly with depth to reach a weak maximum near the top of the thermocline. Little isoline structure of note appeared below the thermocline. The only significant isotherm slopes in the section of Fig. 4 were found at intermediate depths between stations F 799 and F 800 in the south, and between depths of 200 and 700 m in the north from station F 808 to F 809. The latter feature was associated with the only significant geopotential slope found in the survey area. At most stations of the survey a region of relatively weak vertical temperature gradient was found below the summer thermocline layer. In the temperature cross section of Fig. 4 this region was found at a depth of some 200 m at all stations except F 808. Below this region lay the top of the main thermocline layer, at about 300 m, which coincided with the top of the main halocline, the vertical salinity gradient being rather weak between this depth and the surface. This double thermocline structure was also characteristic of

This work is licensed under the Creative Commons Attribution-NonCommercial-NoDerivs 3.0 Unported License.
To view a copy of this license, visit http://creativecommons.org/licenses/by-nc-nd/3.0/

many stations in the adjacent south-east Tasman and north-west survey blocks. Below the deep thermocline the temperature fell, with a steadily decreasing gradient, to reach 2°C at a depth of about 2 km. Below the halocline, salinity decreased with increasing depth to reach a minimum of about 34.5‰ at a depth of some 900 m in the core of the Antarctic Intermediate Water. Salinity in this core layer tended to increase where it approached close to the sea floor (Fig. 7), probably owing to an increase in turbulent vertical mixing, as has been noted for the other survey areas around New Zealand. Beneath the Antarctic Intermediate core, salinity increased slowly to reach some 34.7‰ at a depth of 2 km. No significant difference in the salinity of this Deep Water at a given temperature each side of the Lord Howe Rise was evident (Wyrtki, 1961).

TABLE 2. Mean Vertical Sounding Velocity and Echo Sounding Corrections for station F 800 compared with data for Matthews' (1939) Area No. 42

Depth (m)	F 800		Area 42	
	MSV (m/sec)	Corrn. (m)	MSV (m/sec)	Corrn. (m)
200	1,509.2	+ 1.2	1,504	+ 1
400	1,504.6	+ 1.2	1,499	0
600	1,500.8	+ 0.3	1,496	− 2
800	1,497.8	− 1.1	1,493	− 4
1,000	1,495.2	− 3.1	1,492	− 5
1,200	1,493.2	− 5.4	1,491	− 7
1,400	1,491.9	− 7.7	1,490	− 9
1,600	1,490.9	− 9.6	1,490	−11
1,800	1,490.6	−11.3	1,490	−12
2,000	1,490.4	−12.8	1,489	−14

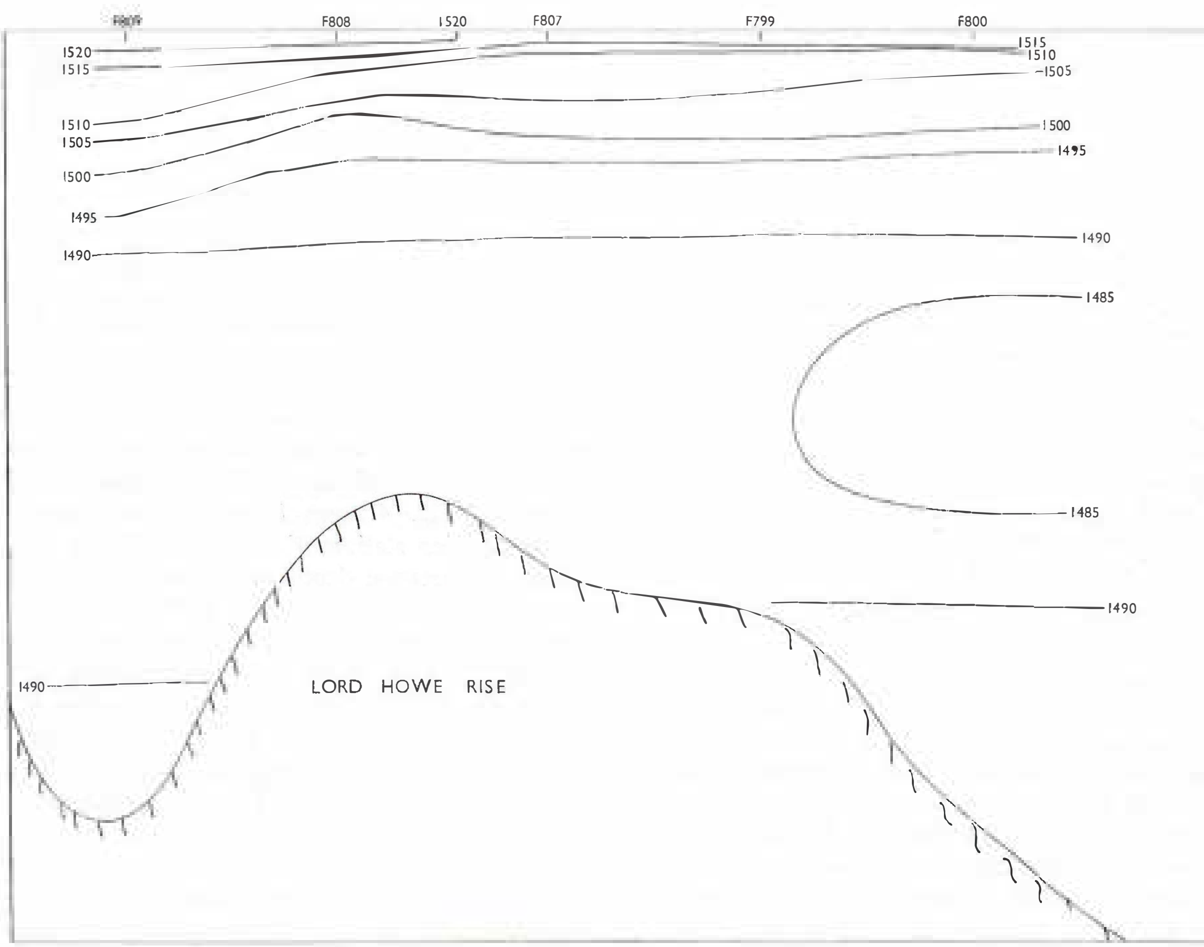

FIG. 9. Vertical cross section of sound velocity (m/sec) across the Lord Howe Rise corresponding to the hydrological sections of Figs. 4 and 5.

This work is licensed under the Creative Commons Attribution-NonCommercial-NoDerivs 3.0 Unported License.
To view a copy of this license, visit http://creativecommons.org/licenses/by-nc-nd/3.0/

DYNAMICS

In terms of the relative geopotential slope of the sea surface (Fig. 8) the dynamical structure of the survey block was very weak indeed. Geostrophic flow was generally from the west with an indication of increasing velocities in the north of the area. This is close to the southern edge of the relatively strong flow of water (defined by the north-west survey) from the East Australian Current running eastwards to the north of New Zealand.

SOUND VELOCITY

In the vertical section of sound velocity (Fig. 9) a weak subsurface maximum was defined at a depth of about 30 m. Below this, velocity decreased with increasing depth to form the minimum of the SOFAR channel at a depth of 1.3 to 1.4 km.

No great differences were found between mean vertical sounding velocities calculated from the survey data and those estimated for the region by Matthews (1939). A comparison of the two sets of figures is presented in Table 2 for station F 800, which provided data from the greatest depth reached by this survey.

ACKNOWLEDGMENTS

The writer is grateful for the assistance of K. B. Lewis, W. Main, R. J. Singleton, and B. R. Stanton, all of the N.Z. Oceanographic Institute, with the field work, and for the willing co-operation of the crew of m.v. *Taranui* under Captain D. K. Matheson. Computing facilities were provided by the Applied Mathematics Division of the DSIR, Wellington. Figures for each of the cruise reports of this hydrological survey series were prepared for publication by the Cartographic Section of DSIR.

This work is licensed under the Creative Commons Attribution-NonCommercial-NoDerivs 3.0 Unported License.
To view a copy of this license, visit http://creativecommons.org/licenses/by-nc-nd/3.0/

REFERENCES

GARNER, D. M. 1967a: Hydrology of the Southern Hikurangi Trench Region. *Bull. N.Z. Dep. scient. ind. Res. 177.*

—— 1967b: Hydrology of the South-east Tasman Sea. *Bull. N.Z. Dep. scient. ind. Res. 181.*

—— 1969a: The Seasonal Range of Sea Temperature on the New Zealand Shelf. *N.Z. Jl mar. Freshwat. Res.* 3: 201–8.

—— 1969b: The Geopotential Topography of the Ocean Surface around New Zealand. *N.Z. Jl mar. Freshwat. Res. 3:* 209–19.

LAFOND, E. C. 1951: Processing Oceanographic Data. *Publs U.S. hydrogr. Off. 614.*

MATTHEWS, D. J. 1939: Tables of the Velocity of Sound in Pure Water and Sea Water for use in Echo Sounding and Sound Ranging. *Publs Admiralty hydrogr. Dep. 282*: 1–151.

RIDGWAY, N. M. (in press): Hydrology of the Southern Kermadec Trench Region. *Bull. N.Z. Dep. scient. ind. Res.*

WILSON, W. D. 1960: Speed of Sound in Sea Water as a Function of Temperature, Pressure and Salinity. *J. acoust. Soc. Am. 32* (*6*): 641–4.

WYRTKI, K. 1961: The Flow of Water into the Deep Sea Basins of the Western South Pacific Ocean. *Aust. J. mar. Freshwat. Res. 12* (*1*): 1–16.

This work is licensed under the Creative Commons Attribution-NonCommercial-NoDerivs 3.0 Unported License.
To view a copy of this license, visit http://creativecommons.org/licenses/by-nc-nd/3.0/

APPENDIX

Numerical Station Data

P is the sampling pressure in decibars. This is numerically nearly equal to the geometric depths in metres. A more accurate conversion using representative mean density figures (LaFond, 1951, p. 8) is as follows:

pressure (*decibars*):	200	400	600	800	1000	1500	2000	2500
depth (*metres*):	199	398	595	793	991	1484	1976	2467

T is the sample temperature in °c × 100.

S is the sample salinity in ‰ × 100.

σ_t is the density reduced to surface pressure isothermally × 100.

σ_{stp} is the *in situ* density × 100.

The "σ" value is derived from the specific gravity, ρ, from the relation $\sigma = (\rho - 1) \times 10^5$.

$\Sigma\Delta D$ is the anomaly of the geopotential distance from the sea surface to the sample depth, in dynamic metres × 100.

C is the *in situ* sound velocity in m/sec × 10.

C_m is the harmonic mean sound velocity between the sea surface and the sample depth, in m/sec × 10.

K is the correction, in metres, to be applied to an echo sounding of a depth corresponding to the depth D on a machine calibrated for a velocity of 1,500 m/sec × 10.

This work is licensed under the Creative Commons Attribution-NonCommercial-NoDerivs 3.0 Unported License.
To view a copy of this license, visit http://creativecommons.org/licenses/by-nc-nd/3.0/

P	T	S	σ_t	σ_{stp}	$\Sigma\Delta D$	C	C_m	K
F 799								
0	1829	3545	2556	2556	0	15179	15179	0
10	1829	3545	2556	2561	2	15180	15179	1
20	1829	3545	2556	2565	5	15182	15180	2
30	1829	3545	2556	2570	7	15183	15181	4
40	1758	3541	2571	2588	10	15164	15179	5
65	1555	3539	2617	2646	15	15107	15162	7
85	1477	3538	2633	2671	19	15086	15147	8
130	1408	3534	2645	2703	26	15069	15123	11
170	1352	3529	2653	2729	32	15057	15109	12
264	1259	3518	2663	2781	47	15040	15087	15
315	1182	3508	2670	2812	54	15020	15078	16
368	1073	3492	2678	2844	62	14990	15067	17
415	980	3479	2684	2871	68	14961	15057	16
469	894	3468	2690	2902	75	14937	15044	14
550	817	3460	2695	2945	85	14920	15027	10
634	760	3454	2699	2987	95	14912	15012	5
700	703	3451	2705	3023	103	14899	15002	1
780	626	3448	2713	3068	112	14882	14991	5-
855	582	3447	2718	3107	120	14876	14981	11-
1095	431	3455	2742	3243	142	14855	14955	33-
F 800								
0	1813	3532	2550	2550	0	15172	15172	0
10	1813	3532	2550	2555	2	15174	15173	1
20	1813	3532	2550	2559	5	15176	15174	2
30	1809	3532	2551	2565	7	15176	15175	3
53	1706	3539	2582	2605	13	15150	15170	6
80	1483	3537	2631	2667	18	15086	15152	8
100	1398	3533	2646	2691	22	15061	15136	9
150	1337	3527	2654	2722	29	15048	15109	11
200	1283	3521	2661	2750	37	15037	15092	12
305	1151	3503	2672	2809	52	15007	15068	14
360	1030	3486	2681	2843	60	14972	15056	13
419	949	3474	2685	2875	67	14950	15043	12
490	871	3463	2689	2911	77	14931	15028	9
569	808	3457	2694	2952	86	14919	15014	5
649	740	3452	2701	2995	96	14905	15001	0
734	663	3448	2708	3042	106	14889	14989	5-
798	593	3446	2716	3079	113	14871	14980	11-
851	529	3445	2723	3112	118	14854	14973	15-
915	476	3445	2729	3148	124	14842	14964	22-
1112	367	3452	2746	3256	141	14831	14941	44-
1500	265	3462	2764	3452	168	14853	14915	85-
1993	210	3469	2774	3684	197	14912	14907	123-
F 801								
0	1769	3539	2566	2566	0	15161	15161	0
7	1769	3539	2566	2570	2	15162	15161	1
17	1769	3539	2566	2574	4	15164	15162	2
22	1766	3539	2567	2577	5	15163	15162	2
47	1713	3537	2579	2599	11	15152	15160	5
76	1506	3533	2623	2657	17	15093	15145	7
100	1477	3533	2629	2674	21	15087	15132	9
150	1346	3528	2653	2721	29	15051	15111	11
190	1299	3522	2658	2743	35	15041	15097	12
300	1192	3508	2669	2803	52	15022	15073	15
362	1101	3496	2676	2839	60	14999	15062	15
407	1005	3481	2681	2865	67	14970	15054	15
460	922	3470	2687	2895	74	14946	15043	13
534	844	3461	2692	2934	83	14929	15028	10
605	782	3456	2698	2972	92	14916	15016	6
719	700	3450	2705	3031	105	14901	14998	1-

This work is licensed under the Creative Commons Attribution-NonCommercial-NoDerivs 3.0 Unported License.
To view a copy of this license, visit http://creativecommons.org/licenses/by-nc-nd/3.0/

P	T	S	σ_t	σ_{stp}	$\Sigma\Delta D$	C	C_m	K
F 801 cont.								
815	639	3447	2710	3081	116	14892	14986	7-
865	555	3445	2720	3114	121	14866	14980	11-
903	502	3445	2726	3139	125	14851	14975	15-
1228	359	3452	2747	3310	153	14846	14941	48-
1592	262	3464	2765	3495	178	14866	14922	83-
1978	220	3471	2774	3677	201	14915	14916	111-
F 802								
0	1725	3526	2567	2567	0	15146	15146	0
10	1713	3523	2568	2572	2	15144	15145	1
20	1702	3521	2569	2578	5	15142	15144	2
30	1699	3521	2570	2583	7	15142	15143	3
50	1678	3524	2577	2599	12	15140	15142	5
75	1497	3534	2626	2659	17	15090	15133	7
100	1420	3533	2642	2686	21	15068	15120	8
150	1337	3527	2654	2722	29	15048	15099	10
225	1283	3520	2660	2761	40	15042	15081	12
331	1169	3504	2670	2818	56	15019	15065	14
395	1059	3489	2678	2856	65	14988	15055	14
470	943	3471	2684	2896	75	14956	15041	13
528	852	3462	2692	2931	82	14930	15031	11
589	780	3456	2698	2965	90	14912	15019	8
686	696	3451	2706	3018	101	14894	15003	1
793	631	3447	2712	3072	113	14886	14987	7-
854	566	3445	2718	3108	120	14869	14979	12-
916	480	3445	2728	3148	126	14845	14971	18-
980	385	3450	2743	3193	131	14816	14962	25-
1147	323	3457	2754	3282	143	14818	14941	45-
F 803								
0	1799	3536	2557	2557	0	15169	15169	0
10	1769	3536	2564	2569	2	15162	15165	1
16	1794	3536	2558	2565	4	15171	15166	2
26	1793	3537	2559	2571	6	15172	15168	3
50	1782	3537	2562	2584	12	15172	15170	6
77	1721	3534	2574	2608	18	15159	15168	9
97	1629	3532	2594	2637	23	15134	15164	11
143	1441	3530	2635	2699	32	15083	15146	14
173	1388	3529	2645	2723	37	15070	15134	15
254	1328	3525	2655	2768	50	15063	15112	19
315	1264	3517	2661	2802	59	15050	15101	21
351	1151	3502	2672	2829	64	15015	15094	22
427	1043	3489	2681	2873	75	14988	15078	22
F 804								
0	1810	3534	2553	2553	0	15172	15172	0
10	1809	3534	2553	2557	2	15173	15173	1
18	1811	3534	2552	2560	4	15175	15173	2
23	1808	3533	2552	2562	6	15174	15174	3
51	1808	3533	2552	2575	13	15179	15175	6
75	1650	3530	2588	2621	18	15137	15170	8
100	1451	3529	2632	2677	23	15078	15154	10
162	1355	3528	2652	2724	33	15058	15121	13
212	1322	3524	2655	2750	41	15054	15105	15
306	1232	3513	2665	2802	55	15037	15087	18
392	1128	3499	2674	2849	68	15013	15073	19
500	1064	3492	2680	2904	83	15007	15060	20

This work is licensed under the Creative Commons Attribution-NonCommercial-NoDerivs 3.0 Unported License.
To view a copy of this license, visit http://creativecommons.org/licenses/by-nc-nd/3.0/

P	T	S	σ_t	σ_{stp}	$\Sigma\Delta D$	C	C_m	K
F 805								
0	1847	3543	2550	2550	0	15184	15184	0
11	1838	3543	2552	2557	3	15183	15183	1
16	1831	3542	2553	2561	4	15182	15183	2
22	1823	3542	2555	2565	5	15180	15182	3
51	1820	3542	2556	2579	13	15184	15182	6
70	1800	3541	2560	2591	17	15181	15182	8
98	1734	3539	2575	2618	24	15166	15180	12
140	1537	3537	2619	2682	32	15112	15168	16
182	1427	3534	2641	2722	40	15085	15152	18
255	1364	3527	2649	2763	52	15075	15131	22
318	1267	3517	2661	2803	62	15051	15117	25
375	1122	3498	2674	2842	70	15008	15104	26
421	1037	3488	2681	2871	77	14984	15092	26

P	T	S	σ_t	σ_{stp}	$\Sigma\Delta D$	C	C_m	K
F 806								
0	1833	3534	2547	2547	0	15178	15178	0
8	1820	3533	2549	2553	2	15176	15177	1
17	1814	3534	2552	2559	4	15176	15177	2
23	1811	3533	2552	2562	6	15175	15176	3
53	1717	3526	2569	2593	13	15152	15169	6
73	1574	3530	2606	2638	17	15112	15159	8
100	1496	3536	2628	2672	22	15093	15144	10
169	1346	3528	2653	2729	34	15055	15115	13
250	1286	3521	2660	2772	46	15048	15094	16
317	1171	3506	2671	2813	56	15016	15081	17
370	1062	3490	2679	2845	64	14986	15070	17
424	968	3477	2685	2876	71	14958	15057	16
498	889	3467	2690	2915	80	14940	15041	14
573	822	3461	2695	2955	90	14927	15027	10
675	740	3454	2702	3008	102	14910	15010	5
744	675	3451	2709	3047	110	14896	15000	0
800	623	3449	2714	3078	116	14885	14993	4-
883	538	3446	2722	3126	124	14863	14981	11-
982	479	3446	2729	3178	134	14855	14969	20-
1233	341	3454	2750	3316	155	14840	14944	46-
1596	254	3465	2767	3499	179	14865	14923	82-
1880	216	3471	2775	3635	195	14896	14917	105-

P	T	S	σ_t	σ_{stp}	$\Sigma\Delta D$	C	C_m	K
F 807								
0	1857	3539	2545	2545	0	15186	15186	0
8	1857	3539	2545	2548	2	15188	15187	1
16	1857	3539	2545	2552	4	15189	15188	2
25	1851	3541	2548	2559	6	15189	15188	3
59	1692	3534	2581	2607	14	15147	15177	7
93	1481	3537	2632	2673	21	15088	15155	10
124	1418	3540	2648	2703	26	15073	15136	11
164	1362	3529	2651	2724	33	15060	15119	13
208	1323	3524	2655	2748	40	15053	15106	15
297	1224	3512	2665	2798	53	15032	15087	17
369	1108	3495	2674	2840	63	15003	15073	18
399	1008	3482	2682	2862	67	14970	15067	18
466	905	3470	2690	2900	76	14942	15051	16
523	840	3463	2694	2931	83	14924	15038	13
589	783	3458	2699	2966	91	14913	15024	10
698	709	3453	2706	3023	104	14901	15006	3
762	643	3450	2712	3059	111	14886	14996	2-
821	590	3449	2718	3093	117	14875	14988	7-
921	540	3449	2725	3145	127	14870	14975	15-
1143	431	3451	2739	3261	148	14863	14954	35-

This work is licensed under the Creative Commons Attribution-NonCommercial-NoDerivs 3.0 Unported License.
To view a copy of this license, visit http://creativecommons.org/licenses/by-nc-nd/3.0/

P	T	S	σ_t	σ_{stp}	$\Sigma\Delta D$	C	C_m	K
F 808								
0	1945	3542	2524	2524	0	15211	15211	0
7	1945	3542	2524	2528	2	15213	15212	1
14	1941	3545	2528	2534	4	15212	15212	2
20	1935	3547	2531	2540	5	15212	15212	3
38	1900	3548	2541	2557	10	15206	15210	5
55	1816	3548	2562	2586	14	15185	15206	8
175	1415	3530	2641	2719	39	15079	15155	18
202	1340	3525	2652	2743	43	15059	15143	19
262	1190	3507	2668	2786	52	15015	15119	21
294	1125	3499	2674	2806	57	14996	15107	21
334	1052	3489	2679	2830	62	14975	15092	20
400	986	3480	2684	2864	71	14962	15071	19
441	937	3473	2687	2886	76	14949	15061	18
480	884	3468	2691	2908	81	14935	15051	16
538	834	3463	2695	2939	88	14925	15038	14
590	781	3459	2700	2968	95	14912	15027	11
F 809								
0	2014	3559	2519	2519	0	15232	15232	0
10	2014	3559	2519	2524	3	15234	15233	2
20	2014	3559	2519	2528	6	15235	15234	3
30	2014	3559	2519	2532	8	15237	15234	5
49	2006	3559	2521	2543	14	15238	15236	8
60	1975	3559	2530	2556	17	15231	15235	9
101	1817	3558	2569	2614	27	15193	15226	15
145	1625	3551	2610	2674	37	15143	15208	20
200	1563	3546	2620	2709	47	15131	15189	25
273	1468	3538	2635	2757	60	15113	15171	31
338	1349	3524	2650	2800	71	15084	15157	35
373	1225	3510	2664	2831	77	15045	15148	37
433	1102	3494	2674	2869	86	15010	15131	38
510	982	3479	2684	2913	96	14978	15110	38
591	895	3469	2690	2957	107	14957	15091	36
654	821	3461	2696	2991	115	14939	15077	33
702	740	3455	2703	3021	121	14915	15066	31
758	671	3451	2709	3054	127	14896	15054	27
812	605	3448	2716	3086	133	14879	15043	23
1088	453	3449	2735	3232	160	14862	14999	1-
1405	308	3459	2757	3401	185	14854	14967	31-
1778	226	3467	2771	3585	208	14882	14946	64-
F 810								
0	2021	3560	2518	2518	0	15234	15234	0
10	2021	3560	2518	2523	3	15236	15235	2
20	2021	3561	2519	2528	6	15237	15236	3
30	2019	3560	2519	2532	8	15238	15236	5
50	2014	3560	2520	2542	14	15240	15237	8
75	1792	3555	2573	2606	20	15182	15229	11
158	1481	3540	2634	2704	37	15098	15182	19
220	1405	3531	2643	2741	48	15082	15156	23
295	1287	3518	2658	2790	60	15054	15134	26
374	1168	3503	2669	2837	72	15025	15114	28
428	1028	3486	2681	2874	79	14982	15100	28
479	920	3472	2689	2905	86	14949	15085	27
529	822	3462	2696	2936	92	14919	15071	25
602	741	3455	2703	2976	101	14898	15051	20
665	679	3452	2709	3012	108	14885	15036	16
739	609	3449	2716	3053	116	14868	15020	10
833	547	3448	2723	3103	125	14859	15002	1
891	512	3449	2728	3135	131	14854	14992	5-
1068	396	3453	2744	3234	146	14836	14968	23-
1236	311	3459	2757	3325	158	14828	14949	42-

This work is licensed under the Creative Commons Attribution-NonCommercial-NoDerivs 3.0 Unported License.
To view a copy of this license, visit http://creativecommons.org/licenses/by-nc-nd/3.0/

P	T	S	σ_t	σ_{stp}	$\Sigma\Delta D$	C	C_m	K
F 811								
0	1920	3535	2526	2526	0	15203	15203	0
5	1919	3535	2526	2528	1	15205	15204	1
10	1918	3535	2526	2531	3	15204	15204	1
18	1916	3535	2527	2535	5	15205	15204	2
31	1899	3536	2532	2545	8	15202	15204	4
58	1738	3541	2576	2601	15	15161	15194	7
82	1528	3532	2617	2654	20	15099	15175	10
130	1405	3530	2643	2701	29	15068	15141	12
181	1357	3528	2651	2732	37	15061	15120	14
229	1299	3521	2658	2760	44	15048	15106	16
279	1213	3510	2666	2791	52	15027	15093	17
330	1112	3497	2675	2823	59	14998	15081	18
373	1043	3487	2680	2848	65	14978	15070	17
430	950	3476	2687	2881	72	14953	15056	16
478	880	3469	2693	2909	78	14934	15045	14
522	850	3465	2694	2931	84	14928	15035	12
615	803	3461	2698	2977	95	14926	15019	8
631	724	3455	2705	2992	97	14896	15016	7
761	665	3451	2710	3056	112	14895	14995	2-
894	527	3449	2726	3134	125	14860	14978	13-
1200	359	3456	2750	3300	151	14842	14945	44-
1520	255	3464	2766	3464	172	14852	14924	77-
F 812								
0	1914	3540	2531	2531	0	15202	15202	0
10	1914	3540	2531	2535	3	15204	15203	1
20	1914	3541	2532	2541	5	15205	15204	3
30	1903	3540	2534	2547	8	15204	15204	4
50	1805	3540	2558	2580	13	15179	15199	7
70	1592	3538	2608	2639	17	15118	15185	9
90	1468	3537	2635	2675	21	15083	15166	10
110	1398	3533	2646	2696	24	15063	15149	11
160	1351	3527	2652	2723	32	15055	15121	13
289	1249	3514	2662	2791	52	15041	15088	17
369	1117	3498	2675	2841	64	15006	15074	18
420	998	3483	2684	2874	71	14970	15063	18
466	921	3474	2690	2901	77	14948	15053	16
532	832	3467	2699	2940	85	14923	15038	14
F 813								
0	1951	3538	2520	2520	0	15212	15212	0
10	1950	3538	2520	2525	3	15214	15213	1
20	1948	3538	2521	2529	6	15215	15213	3
30	1939	3538	2523	2536	8	15214	15214	4
47	1937	3538	2523	2544	13	15216	15214	7
68	1653	3541	2596	2626	18	15137	15203	9
85	1530	3539	2622	2660	21	15102	15186	11
146	1390	3530	2646	2711	32	15066	15143	14
200	1300	3520	2657	2746	40	15043	15119	16
281	1180	3505	2668	2795	52	15015	15093	17
358	1079	3492	2677	2838	63	14990	15074	18
417	1005	3483	2683	2871	71	14972	15060	17
495	929	3475	2690	2913	81	14956	15045	15
551	882	3470	2693	2942	88	14946	15035	13
602	824	3464	2698	2970	95	14931	15027	11
660	769	3460	2703	3002	102	14919	15018	8
707	692	3456	2710	3032	107	14897	15011	5
755	620	3453	2718	3062	112	14876	15003	1
1046	443	3452	2738	3217	139	14852	14964	25-

This work is licensed under the Creative Commons Attribution-NonCommercial-NoDerivs 3.0 Unported License.
To view a copy of this license, visit http://creativecommons.org/licenses/by-nc-nd/3.0/

P	T	S	σ_t	σ_{stp}	$\Sigma\Delta D$	C	C_m	K
F 814								
0	1987	3549	2519	2519	0	15223	15223	0
5	1983	3549	2520	2522	1	15224	15224	1
10	1974	3546	2520	2524	3	15221	15223	1
21	1961	3543	2521	2530	6	15219	15221	3
34	1959	3545	2523	2538	9	15222	15221	5
50	1767	3540	2568	2590	14	15168	15213	7
73	1570	3538	2613	2645	18	15112	15190	9
100	1441	3536	2640	2684	23	15075	15164	11
150	1375	3529	2648	2715	31	15061	15132	13
244	1269	3517	2660	2770	46	15040	15100	16
310	1159	3503	2671	2810	56	15012	15084	17
372	1050	3490	2681	2848	64	14981	15070	17
430	973	3479	2685	2879	72	14962	15056	16
478	867	3467	2693	2910	78	14929	15045	14
584	793	3459	2698	2963	91	14917	15023	9
640	736	3455	2703	2994	97	14903	15013	5
727	667	3451	2710	3041	107	14889	14999	1-
789	611	3450	2717	3076	114	14878	14990	5-
982	510	3450	2729	3177	133	14868	14967	22-
1072	429	3452	2740	3230	141	14849	14958	30-
1420	287	3461	2761	3412	167	14849	14931	65-
F 815								
0	2014	3547	2510	2510	0	15231	15231	0
11	2013	3547	2510	2515	3	15232	15231	2
18	2010	3547	2511	2519	5	15233	15232	3
25	1996	3545	2513	2524	7	15230	15232	4
43	1976	3543	2517	2536	12	15226	15230	7
68	1832	3539	2551	2581	19	15190	15222	10
82	1643	3536	2594	2631	22	15135	15212	12
124	1405	3532	2644	2700	30	15068	15174	14
245	1304	3521	2657	2766	49	15052	15118	19
304	1196	3506	2666	2802	58	15023	15102	21
327	1089	3493	2676	2823	61	14988	15095	21
385	1003	3482	2683	2856	69	14965	15077	20
454	913	3471	2689	2894	78	14942	15058	18
512	847	3464	2694	2926	85	14925	15044	15
557	786	3458	2699	2951	91	14909	15034	13
600	733	3454	2703	2976	96	14895	15024	10
659	656	3450	2711	3011	102	14874	15012	5
705	619	3449	2715	3036	107	14867	15002	1
851	504	3449	2729	3118	122	14844	14977	13-
1200	331	3458	2754	3306	150	14830	14936	51-
F 816								
0	2022	3525	2491	2491	0	15230	15230	0
5	2022	3525	2491	2494	2	15232	15231	1
13	2022	3525	2491	2497	4	15232	15231	2
19	2013	3524	2493	2501	6	15231	15231	3
44	1980	3522	2500	2519	13	15226	15230	7
64	1794	3532	2555	2583	19	15178	15221	9
87	1557	3533	2612	2650	24	15110	15201	12
119	1419	3533	2642	2695	30	15071	15171	14
187	1884	3525	2527	2609	45	15222	15162	20
240	1268	3518	2661	2769	56	15040	15155	25
307	1191	3507	2668	2806	66	15022	15128	26
361	1097	3495	2676	2838	73	14997	15110	27
397	1028	3487	2682	2861	78	14978	15099	26
458	951	3478	2688	2895	86	14958	15081	25
536	876	3470	2694	2936	96	14942	15062	22

This work is licensed under the Creative Commons Attribution-NonCommercial-NoDerivs 3.0 Unported License.
To view a copy of this license, visit http://creativecommons.org/licenses/by-nc-nd/3.0/

P	T	S	σ_t	σ_{stp}	$\Sigma\Delta D$	C	C_m	K
F 816 cont.								
580	828	3465	2698	2960	101	14930	15052	20
633	761	3460	2704	2991	108	14913	15041	17
720	699	3456	2709	3036	118	14903	15025	12
877	589	3452	2721	3120	134	14884	15001	1
F 817								
0	1948	3525	2511	2511	0	15210	15210	0
7	1984	3525	2501	2504	2	15221	15216	1
15	1983	3525	2502	2508	4	15223	15219	2
27	1977	3525	2503	2515	8	15223	15221	4
47	1952	3523	2508	2529	14	15219	15221	7
69	1710	3530	2574	2604	20	15153	15210	10
95	1556	3542	2619	2661	25	15113	15189	12
112	1449	3536	2638	2688	28	15080	15174	13
151	1387	3530	2646	2714	34	15065	15148	15
264	1330	3524	2654	2771	52	15065	15112	20
337	1249	3514	2662	2813	64	15047	15100	22
354	1157	3503	2671	2830	66	15018	15097	23
413	1045	3488	2680	2866	74	14986	15083	23
491	967	3479	2686	2908	85	14969	15066	22
563	891	3472	2693	2948	94	14951	15053	20
623	882	3465	2689	2970	102	14958	15043	18
682	751	3460	2705	3014	109	14917	15034	15
723	704	3457	2710	3038	114	14905	15027	13
773	646	3454	2715	3067	119	14890	15018	9
1039	482	3451	2733	3207	145	14866	14982	12-
1405	297	3462	2761	3405	173	14850	14950	47-
F 818								
0	1960	3532	2513	2513	0	15214	15214	0
9	1960	3532	2513	2517	3	15216	15215	1
17	1960	3534	2514	2522	5	15217	15216	2
24	1945	3536	2520	2530	7	15214	15216	3
45	1928	3536	2524	2544	13	15214	15215	6
62	1814	3535	2552	2580	17	15183	15210	9
82	1435	3535	2640	2677	21	15070	15190	10
128	1412	3533	2643	2701	29	15070	15147	13
190	1369	3526	2647	2732	39	15065	15121	15
262	1258	3515	2661	2778	50	15039	15102	18
313	1171	3504	2669	2810	58	15016	15090	19
361	1097	3495	2676	2838	64	14997	15079	19
414	1004	3485	2685	2871	72	14970	15066	18
498	923	3475	2691	2915	82	14954	15049	16
547	857	3469	2696	2944	88	14936	15039	14
592	802	3464	2701	2969	94	14921	15031	12
654	716	3458	2709	3006	101	14898	15019	8
707	659	3455	2714	3036	107	14884	15010	5
900	550	3452	2726	3136	126	14872	14981	11-
1100	440	3454	2740	3243	144	14859	14960	29-
F 819								
0	1896	3535	2532	2532	0	15197	15197	0
11	1896	3535	2532	2537	3	15198	15197	1
19	1896	3535	2532	2540	5	15200	15198	3
20	1893	3535	2532	2541	5	15199	15198	3
46	1892	3534	2532	2552	12	15203	15200	6
66	1595	3534	2604	2633	17	15119	15188	8
120	1416	3533	2643	2696	27	15070	15146	12
225	1329	3525	2655	2755	44	15058	15108	16
287	1238	3514	2664	2793	53	15036	15094	18
306	1158	3503	2671	2808	56	15010	15090	18

This work is licensed under the Creative Commons Attribution-NonCommercial-NoDerivs 3.0 Unported License.
To view a copy of this license, visit http://creativecommons.org/licenses/by-nc-nd/3.0/

P	T	S	σ_t	σ_{stp}	$\Sigma\Delta D$	C	C_m	K
F 819 cont.								
358	1070	3492	2679	2840	63	14987	15077	18
411	973	3481	2687	2872	70	14959	15063	17
491	906	3473	2692	2914	80	14946	15045	15
542	864	3468	2694	2940	86	14937	15035	13
619	812	3464	2699	2980	96	14930	15022	9
683	758	3460	2704	3014	103	14920	15013	6
790	657	3454	2714	3073	115	14897	14999	1-
895	579	3453	2723	3131	126	14882	14986	8-
1190	372	3455	2748	3293	152	14845	14955	35-

This work is licensed under the Creative Commons Attribution-NonCommercial-NoDerivs 3.0 Unported License.
To view a copy of this license, visit http://creativecommons.org/licenses/by-nc-nd/3.0/

MEMOIRS OF THE NEW ZEALAND OCEANOGRAPHIC INSTITUTE

Memoir No.	Year	Title
[1]	1955	Bibliography of New Zealand Oceanography, 1949–1953. By N.Z. OCEANOGRAPHIC COMMITTEE. *N.Z. Dep. scient. ind. Res. geophys. Mem. 4.*
[2]	1957	General Account of the Chatham Islands 1954 Expedition. By G. A. KNOX. *Bull. N.Z. Dep. scient. ind. Res. 122.*
3	1959	Contributions to Marine Microbiology. Compiled by T. M. SKERMAN. *Inf. Ser. N.Z. Dep. scient. ind. Res. 22.*
4	1960	Biological Results of the Chatham Islands 1954 Expedition. Part 1. Decapoda Brachyura, by R. K. DELL; Cumacea by N. S. JONES; Decapoda Natantia, by J. C. YALDWYN. *Bull. N.Z. Dep. scient. ind. Res. 139(1).*
5	1960	Biological Results of the Chatham Islands 1954 Expedition. Part 2. Archibenthal and Littoral Echinoderms. By H. BARRACLOUGH FELL. *Bull. N.Z. Dep. scient. ind. Res. 139(2).*
6	1960	Biological Results of the Chatham Islands 1954 Expedition. Part 3. Polychaeta Errantia. By G. A. KNOX. *Bull. N.Z. Dep. scient. ind. Res. 139(3).*
7	1960	Biological Results of the Chatham Islands 1954 Expedition. Part 4. Marine Mollusca, by R. K. DELL; Sipunculoidea, by S. J. EDWARDS. *Bull. N.Z. Dep. scient. ind. Res. 139(4).*
8	1961	Hydrology of New Zealand Coastal Waters, 1955. By D. M. GARNER. *Bull. N.Z. Dep. scient. ind. Res. 138.*
9	1962	Analysis of Hydrological Observations in the New Zealand Region, 1874–1955. By D. M. GARNER. *Bull. N.Z. Dep. scient. ind. Res. 144.*
10	1961	Hydrology of Circumpolar Waters South of New Zealand. By R. W. BURLING. *Bull. N.Z. Dep. scient. ind. Res. 143.*
11	1964	Bathymetry of the New Zealand Region. By J. W. BRODIE. *Bull. N.Z. Dep. scient. ind. Res. 161.*
12	1965	Hydrology of New Zealand Offshore Waters. By D. M. GARNER and N. M. RIDGWAY. *Bull. N.Z. Dep. scient. ind. Res. 162.*
13	1961	Biological Results of the Chatham Islands 1954 Expedition. Part 5. Porifera: Demospongiae, by PATRICIA R. BERGQUIST; Porifera: Keratosa, by PATRICIA R. BERGQUIST; Crustacea Isopoda: Bopyridae, by RICHARD B. PIKE; Crustacea Isopoda: Serolidae, by D. E. HURLEY; Hydroida, by PATRICIA M. RALPH. *Bull. N.Z. Dep. scient. ind. Res. 139(5).*
14	1963	Submarine Morphology East of the North Island, New Zealand. By H. M. PANTIN. *Bull. N.Z. Dep. scient. ind. Res. 149.*
15	In prep.	Marine Geology of Cook Strait. By J. W. BRODIE. *Bull. N.Z. Dep. scient. ind. Res.*
16	1963	Bibliography of New Zealand Marine Zoology 1769–1899. By DOROTHY FREED. *Bull. N.Z. Dep. scient. ind. Res. 148.*
17	1965	Studies of a Southern Fiord. By T. M. SKERMAN (Ed.) *Bull. N.Z. Dep. scient. ind. Res. 157.*
18	1961	The Fauna of the Ross Sea. Part 1. Ophiuroidea. By H. BARRACLOUGH FELL. *Bull. N.Z. Dep. scient. ind. Res. 142.*
19	1962	The Fauna of the Ross Sea. Part 2. Scleractinian Corals. By DONALD F. SQUIRES. *Bull. N.Z. Dep. scient. ind. Res. 147.*
20	1963	*Flabellum rubrum* (Quoy and Gaimard). By DONALD F. SQUIRES. *Bull. N.Z. Dep. scient. ind. Res. 154.*
21	1963	The Fauna of the Ross Sea. Part 3. Asteroidea. By HELEN E. SHEARBURN CLARK. *Bull. N.Z. Dep. scient. ind. Res. 151.*
22	1964	The Marine Fauna of New Zealand: Crustacea Brachyura. By E. W. BENNETT, *Bull. N.Z. Dep. scient. ind. Res. 153.*
23	1963	The Marine Fauna of New Zealand: Crustaceans of the Order Cumacea. By N. S. JONES, *Bull. N.Z. Dep. scient. ind. Res. 152.*
24	1964	A Bibliography of the Oceanography of the Tasman and Coral Seas, 1860–1960. By BETTY N. KREBS. *Bull. N.Z. Dep. scient. ind. Res. 156.*
25	1965	A Foraminiferal Fauna from the Western Continental Shelf, North Island, New Zealand. By R. H. HEDLEY, C. M. HURDLE, and I. D. J. BURDETT. *Bull. N.Z. Dep. scient. ind. Res. 163.*
26	1964	Sediments of Chatham Rise. By ROBERT M. NORRIS. *Bull. N.Z. Dep. scient. ind. Res. 159.*
27	1965	The Fauna of the Ross Sea. Part 4. Mysidacea. By OLIVE S. TATTERSALL. Part 5. Sipunculoidea. By S. J. EDMONDS. *Bull. N.Z. Dep. scient. ind. Res. 167.*
28	1966	Sedimentation in Hawke Bay. By H. M. PANTIN. *Bull. N.Z. Dep. scient. ind. Res. 171.*
29	1964	Biological Results of the Chatham Islands 1954 Expedition. Part 6. Scleractinia. By D. F. SQUIRES. *Bull. N.Z. Dep. scient. ind. Res. 139 (6).*

This work is licensed under the Creative Commons Attribution-NonCommercial-NoDerivs 3.0 Unported License.
To view a copy of this license, visit http://creativecommons.org/licenses/by-nc-nd/3.0/

Memoir No.	*Year*	*Title*
30	1966	Geology and Geomagnetism of the Bounty Region east of the South Island, New Zealand. By D. C. KRAUSE. *Bull. N.Z. Dep. scient. ind. Res. 170.*
31	In prep.	Marine Biology, Hydrology, Physiography of Manihiki Atoll, Cook Islands, Compiled by C. MCCANN and J. S. BULLIVANT. *Bull. N.Z. Dep. scient. ind. Res.*
32	1967	The Fauna of the Ross Sea. Part 5. General Accounts, Station Lists, and Benthic Ecology. By JOHN S. BULLIVANT and JOHN H. DEARBORN. *Bull. N.Z. Dep. scient. ind. Res. 176.*
33	1967	The Submarine Geology of Foveaux Strait. By D. J. CULLEN. *Bull. N.Z. Dep. scient. ind. Res. 184.*
34	In prep.	Benthic Ecology of Foveaux Strait. By E. W. DAWSON. *Bull. N.Z. Dep. scient. ind. Res.*
35	1966	The Marine Fauna of New Zealand: Spider Crabs, Family Majidae (Crustacea Brachyura). By D. J. GRIFFIN. *Bull. N.Z. Dep. scient. ind. Res. 172.*
36	1967	Water Masses and Fronts in the Southern Ocean South of New Zealand. By TH. J. HOUTMAN. *Bull. N.Z. Dep. scient. ind. Res. 174.*
37	1968	The Marine Fauna of New Zealand: Porifera, Demospongiae. Part 1. Tetractinomorpha and Lithistida. By PATRICIA R. BERGQUIST. *Bull. N·Z. Dep. scient. ind. Res. 188*
38	1967	The Marine Fauna of New Zealand: Intertidal Foraminifera of the *Corallina officinalis* zone. By R. H. HEDLEY, C. M. HURDLE and I. D. J. BURDETT. *Bull. N.Z. Dep. scient. ind. Res. 180.*
39	1967	Hydrology of the Southern Hikurangi Trench Region. By D. M. GARNER. *Bull. N.Z. Dep. scient. ind. Res. 177.*
40	1967	Sediments of the Western Shelf, North Island, New Zealand. By J. C. MCDOUGALL and J. W. BRODIE. *Bull. N.Z. Dep. scient. ind. Res. 179.*
41	1967	Bathymetric and Geological Structure of the North-western Tasman Sea – Coral Sea – South Solomon Sea Area of the South-western Pacific Ocean. By DALE C. KRAUSE. *Bull. N.Z. Dep. scient. ind. Res. 183.*
42	1968	The Echinozoan Fauna of the New Zealand Subantarctic Islands, Macquarie Island and the Chatham Rise. By D. L. PAWSON. *Bull. N.Z. Dep. scient. ind. Res. 187.*
43	1967	The Marine Fauna of New Zealand. Scleractinian Corals. By D. F. SQUIRES and I. W. KEYES. *Bull. N.Z. Dep. scient. ind. Res. 185.*
44	1967	A Checklist of Recent New Zealand Foraminifera. By J. V. EADE. *Bull. N.Z. Dep. scient. ind. Res. 182.*
45	In press	A Key to the Recent Genera of the Foraminifera. By K. B. LEWIS. *Bull. N.Z. Dep. scient. ind. Res. 196.*
46	1968	The Fauna of the Ross Sea. Part 6. Ecology and Distribution of Foraminifera. By J. P. KENNETT. *Bull. N.Z. Dep. scient. ind. Res. 186.*
47	1969	An Outline Distribution of the New Zealand Shelf Fauna. Echinoidea. By D. G. MCKNIGHT. *Bull. N.Z. Dep. scient. ind. Res. 195.*
48	1967	Hydrology of the South-east Tasman Sea. By D. M. GARNER. *Bull. N.Z. Dep. scient. ind. Res. 181.*
49	1969	The Fauna of the Ross Sea. Part 7. Pycnogonida 1: Colossendeidae, Pycnogonidae, Endeidae and Ammotheidae. By W. G. FRY and J. W. HEDGPETH. *Bull. N.Z. Dep. scient. ind. Res. 198.*
50	1969	Marine Geology of the New Zealand Subantarctic Sea Floor. By C. P. SUMMERHAYES. *Bull. N.Z. Dep. scient. ind. Res. 190.*
51	In press	The Marine Fauna of New Zealand: Porifera, Demospongiae. Part 2. Axinellidae and Halichondrida. By PATRICIA R. BERGQUIST. *Bull. N.Z. Dep. scient. ind. Res. 197.*
52	In press	The Marine Fauna of New Zealand: Sea Cucumbers (Echinodermata; Holothuroidea). By D. L. PAWSON. *Bull. N.Z. Dep. scient. ind. Res.*
53	In press	Plankton of Hauraki Gulf. By J. B. JILLETT. *Bull. N·Z. Dep. scient. ind. Res.*
54	In press	Studies on New Zealand Plankton. Part 1. Pelagic Copepoda from New Zealand with a key to Pelagic Genera. Part 2. Plankton and Environmental Variation (Kaikoura 1964–65). By J. M. BRADFORD. *Bull. N.Z. Dep. scient. ind. Res.*
55	In press	Bay Head Sand Beaches of Banks Peninsula, New Zealand. By P. R. DINGWALL. *Bull. N.Z. Dep. scient. ind. Res.*
56	In press	Hydrology of the Southern Kermadec Trench Region. By N. M. RIDGWAY. *Bull. N.Z. Dep. scient. ind. Res.*
57	In press	Biological Results of the Chatham Islands 1954 Expedition. Part 7. Chelostomate Bryozoa. By G. H. UTTLEY and J. S. BULLIVANT. *Bull. N.Z. Dep. scient. ind. Res.*

A. R. SHEARER, GOVERNMENT PRINTER, WELLINGTON, NEW ZEALAND—1970

1,400/2/69—60023 A

This work is licensed under the Creative Commons Attribution-NonCommercial-NoDerivs 3.0 Unported License.
To view a copy of this license, visit http://creativecommons.org/licenses/by-nc-nd/3.0/

A. R. SHEARER, GOVERNMENT PRINTER,
WELLINGTON, NEW ZEALAND—1970

cc BY NC ND